Electronic Supporting Information

for

A rigid anionic Janus bis(NHC) – new opportunities in NHC chemistry

Nabila Rauf Naz,[a] Gregor Schnakenburg,[a] Zsolt Kelemen,[b] Dalma Gál,[b] László Nyulászi,[b]* René T. Boeré,[c]* and Rainer Streubel[a]*

Table of Contents

1. NMR spectra of all new compounds

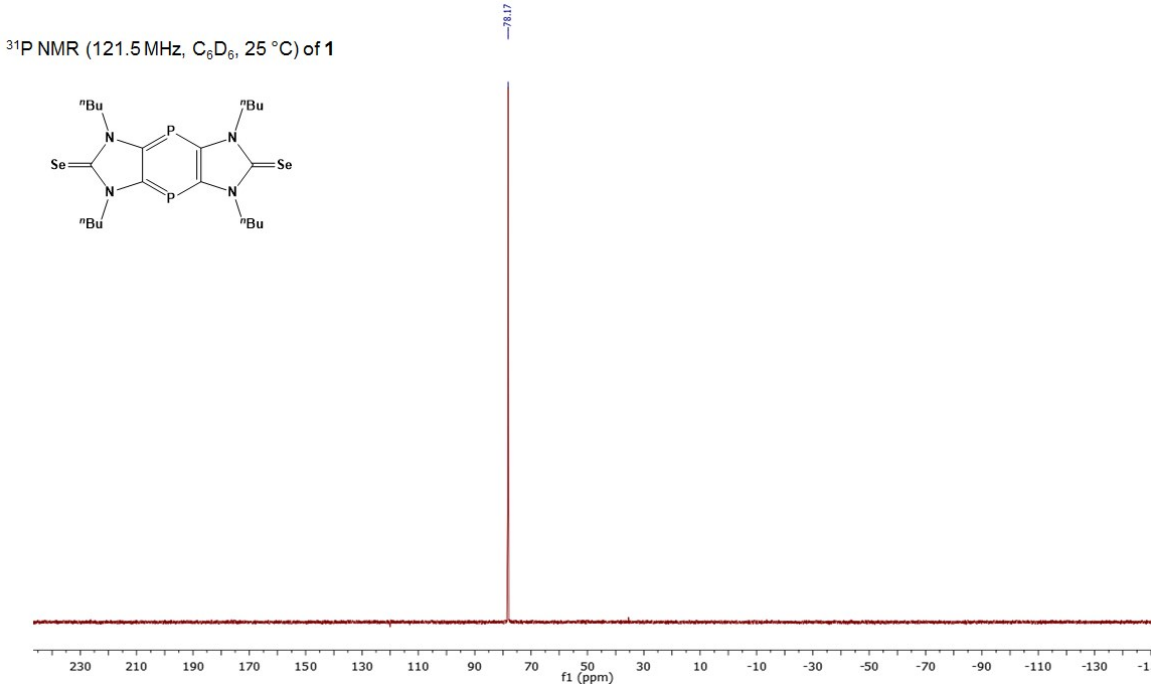

Figure S1: ^{31}P NMR spectrum of compound **1**

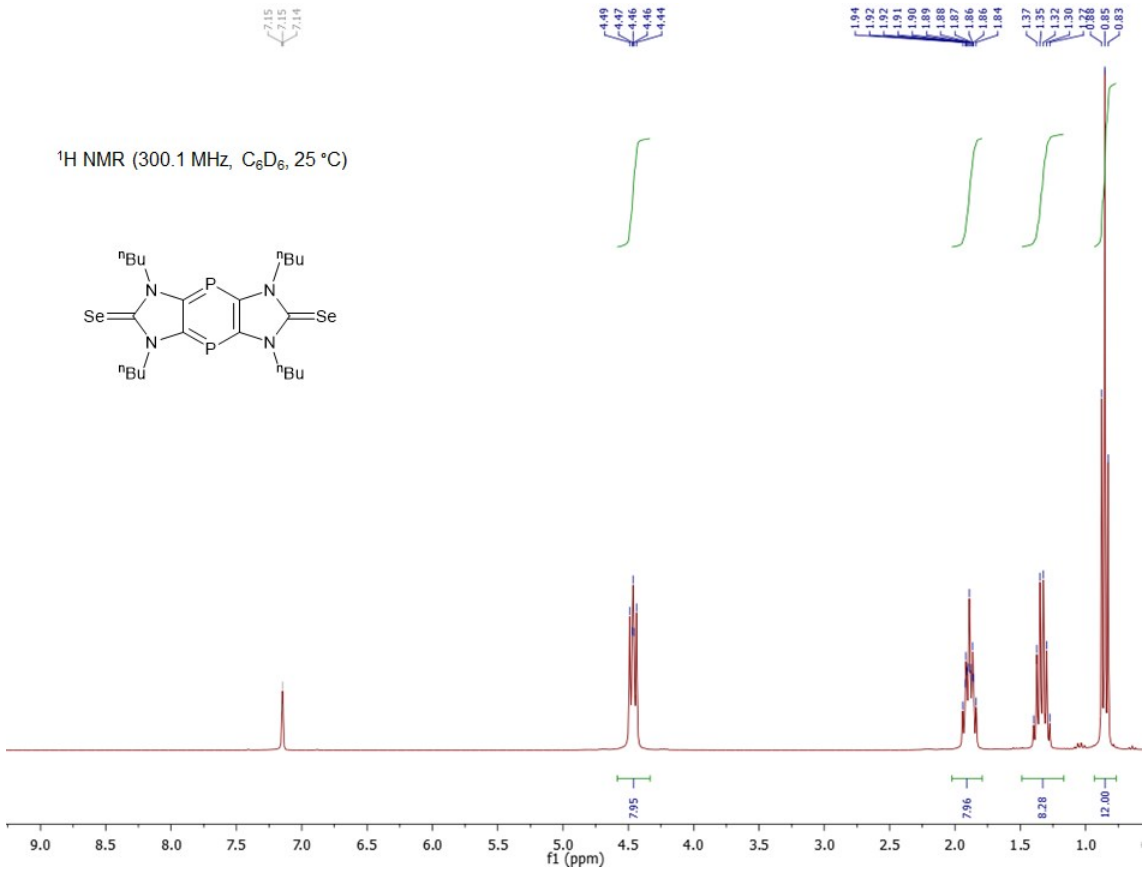

Figure S2: ^{1}H NMR spectrum of compound **1**

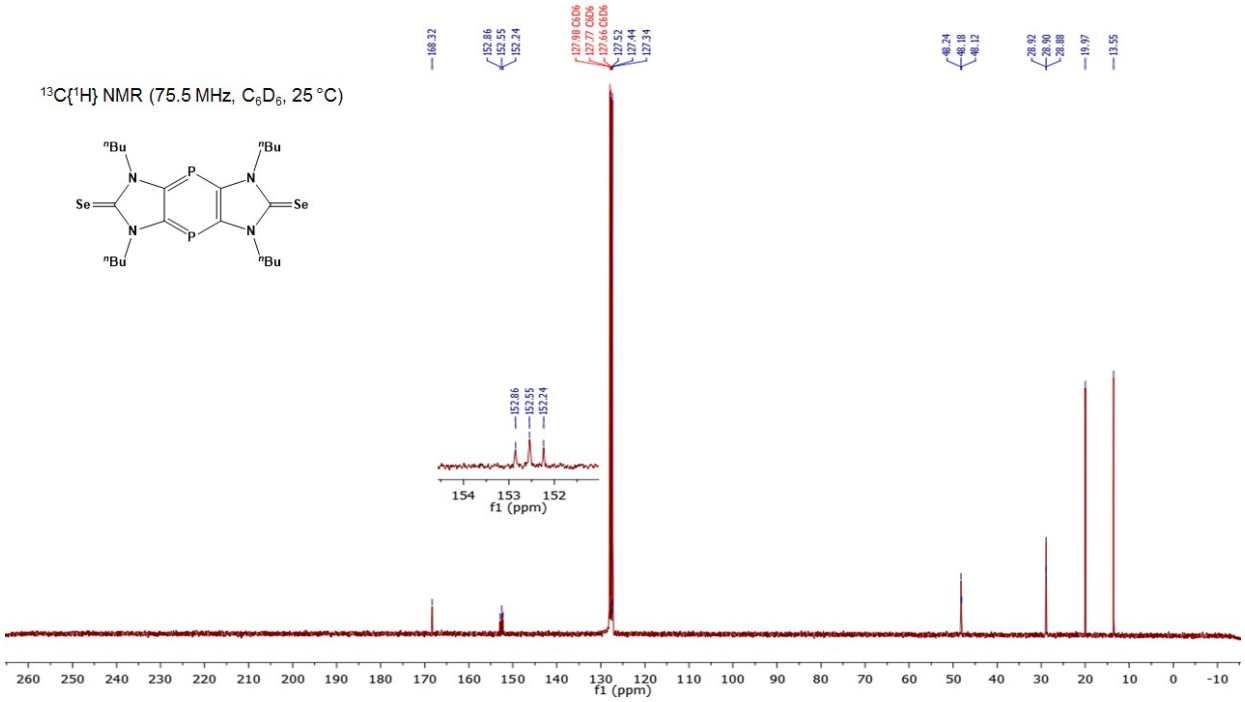

Figure S3: $^{13}C\{^{1}H\}$ NMR spectrum of compound **1**

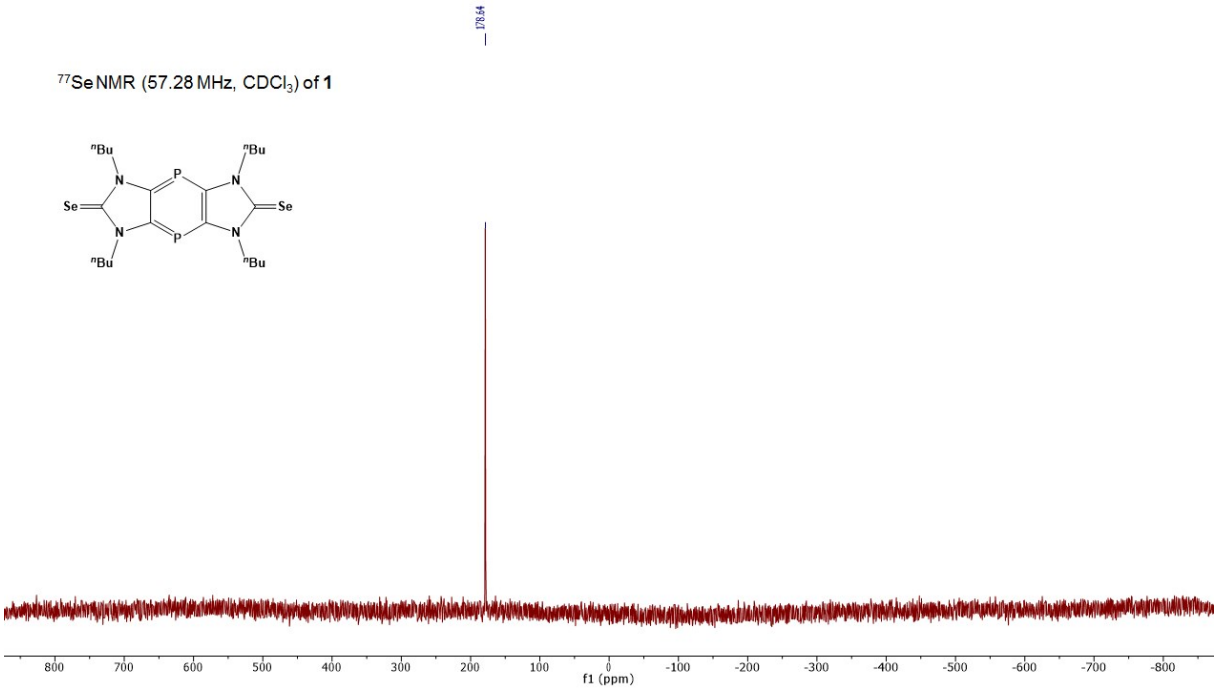

Figure S4: ^{77}Se NMR spectrum of compound **1**

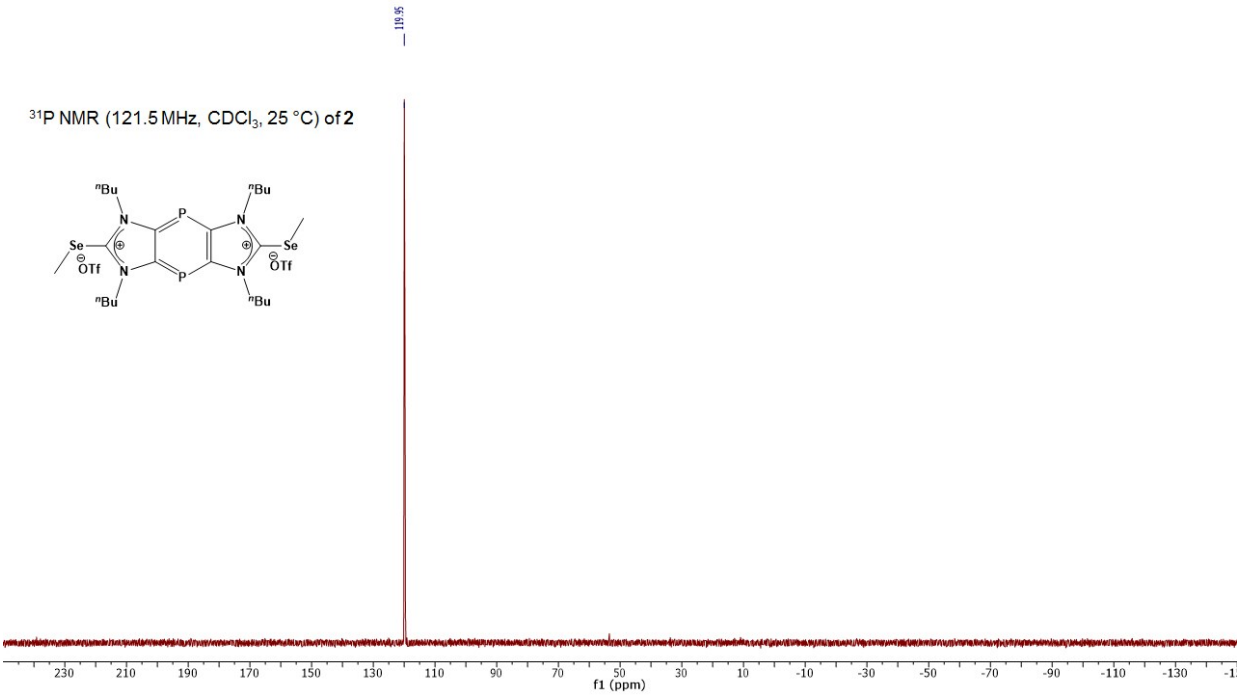

Figure S5: ^{31}P NMR spectrum of compound **2**

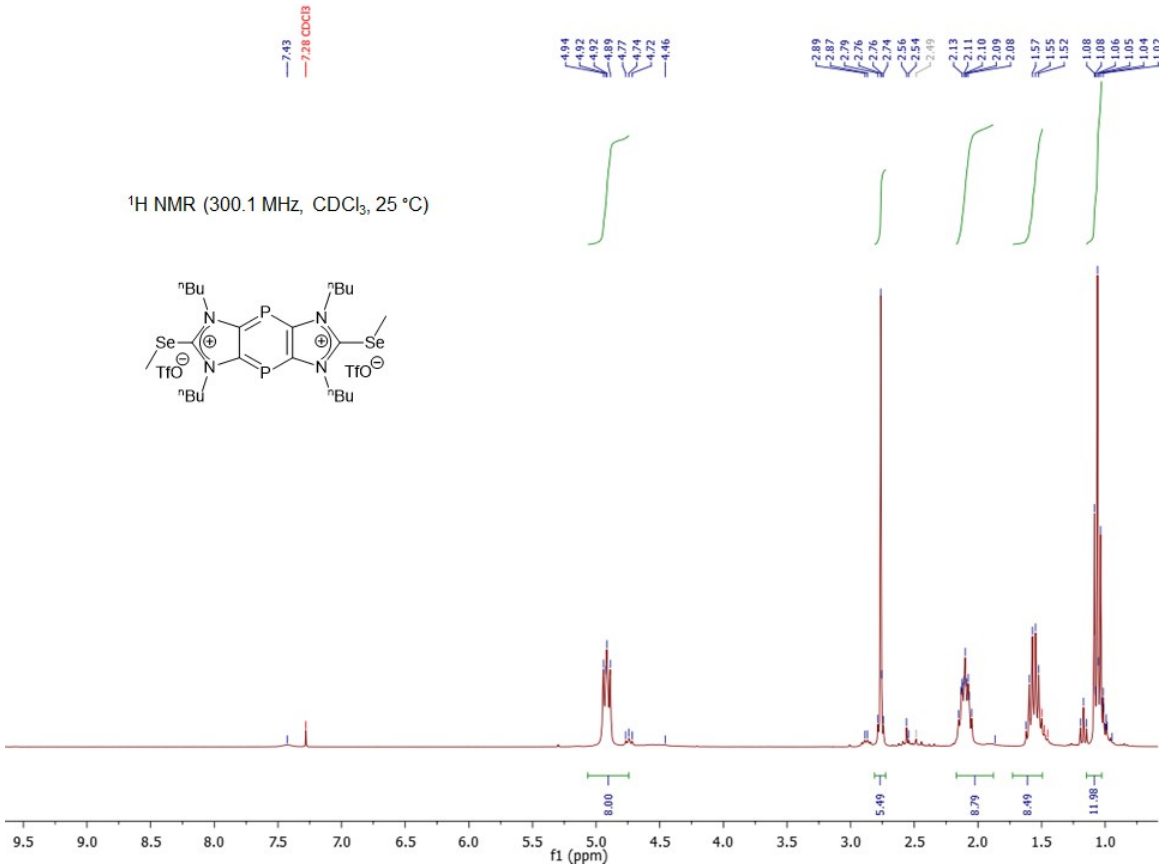

Figure S6: ^{1}H NMR spectrum of compound **2**

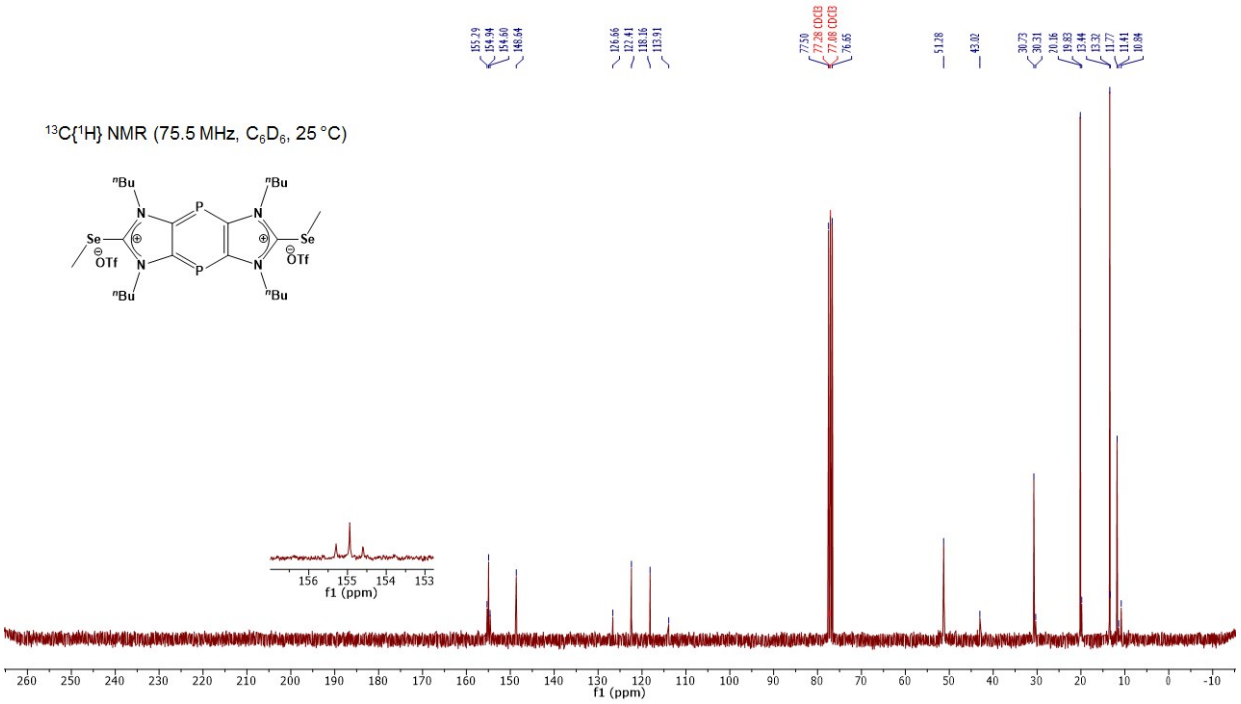

Figure S7: $^{13}C\{^{1}H\}$ NMR spectrum of compound **2**

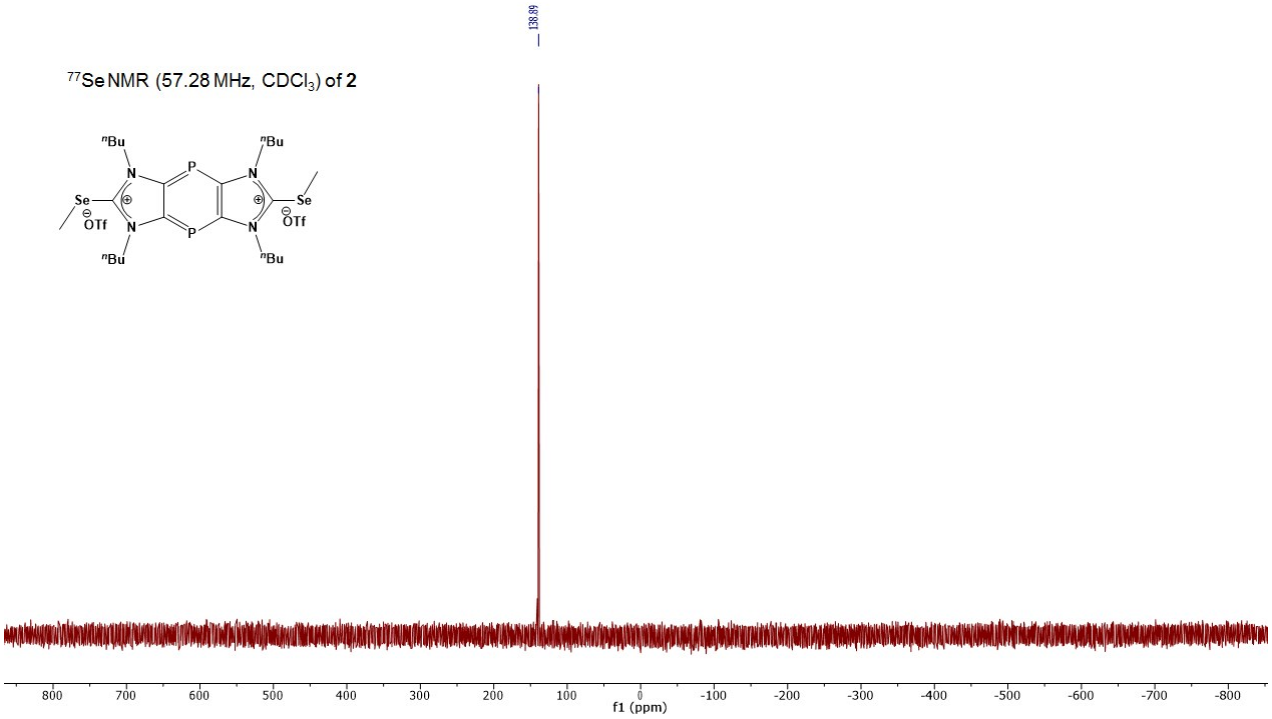

Figure S8: ^{77}Se NMR spectrum of compound **2**

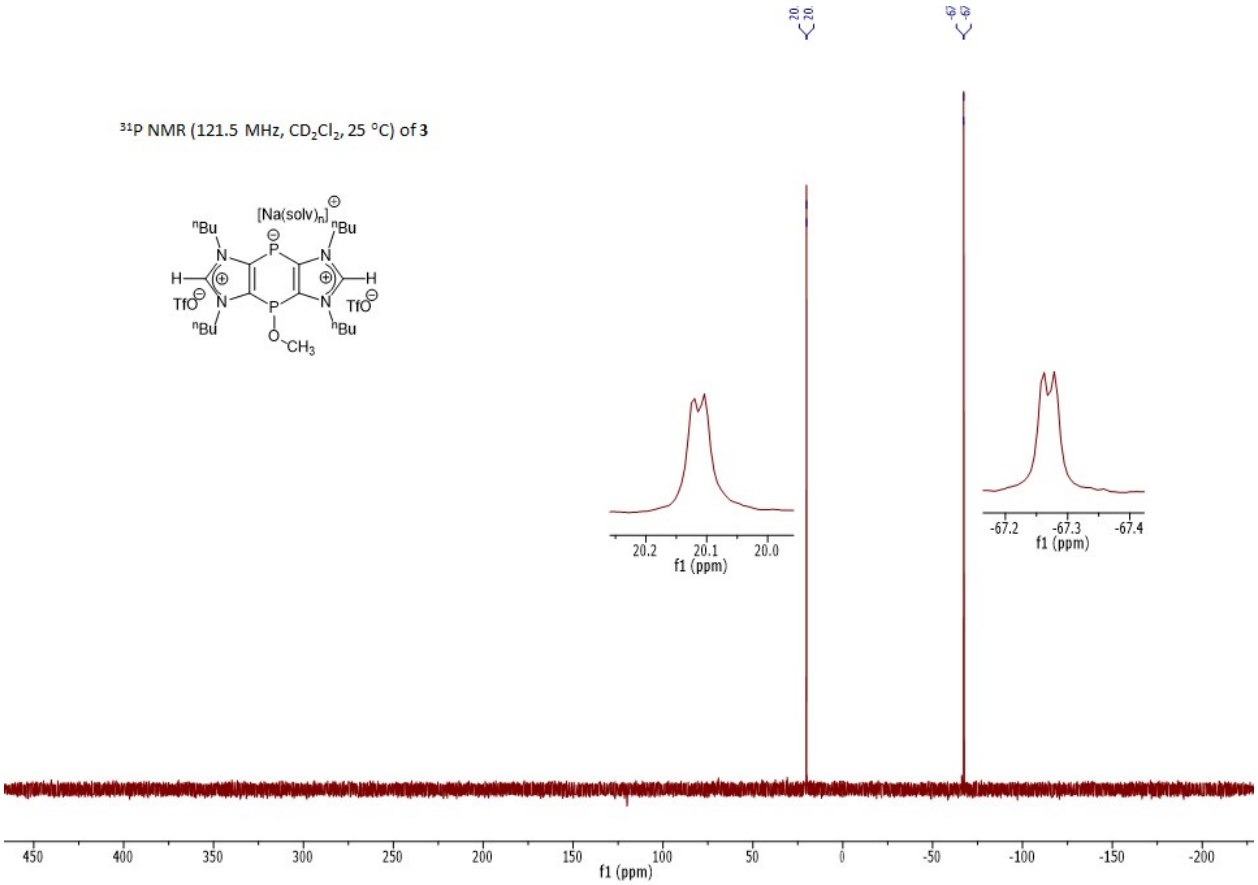

Figure S9: ^{31}P NMR spectrum of compound **3**

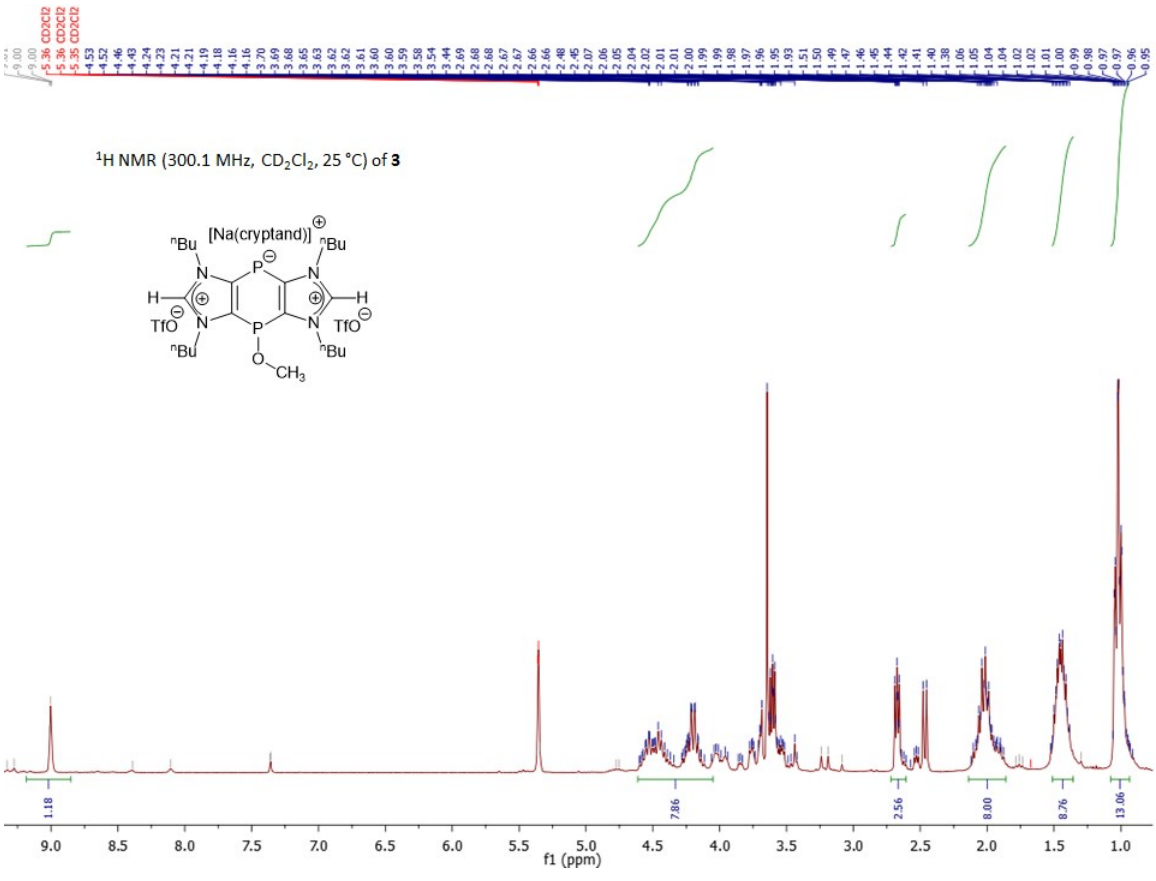

Figure S10: ^{1}H NMR spectrum of compound **3**

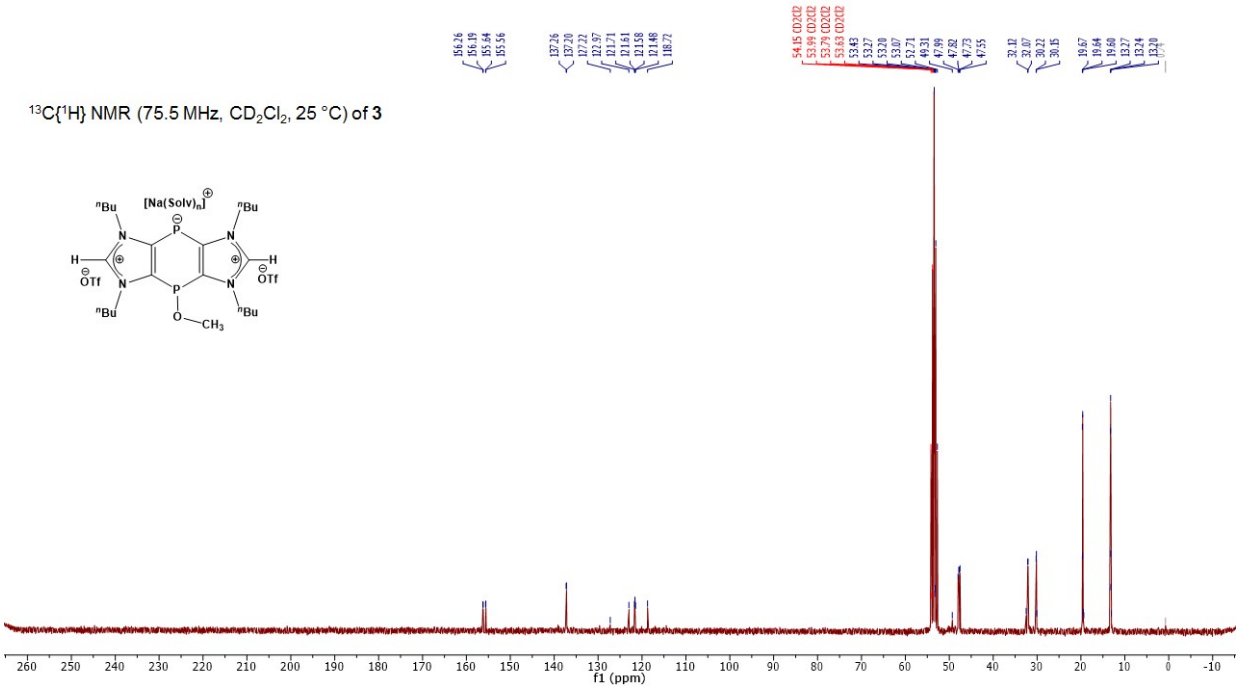

Figure S11: $^{13}C\{^{1}H\}$ NMR spectrum of compound **3**

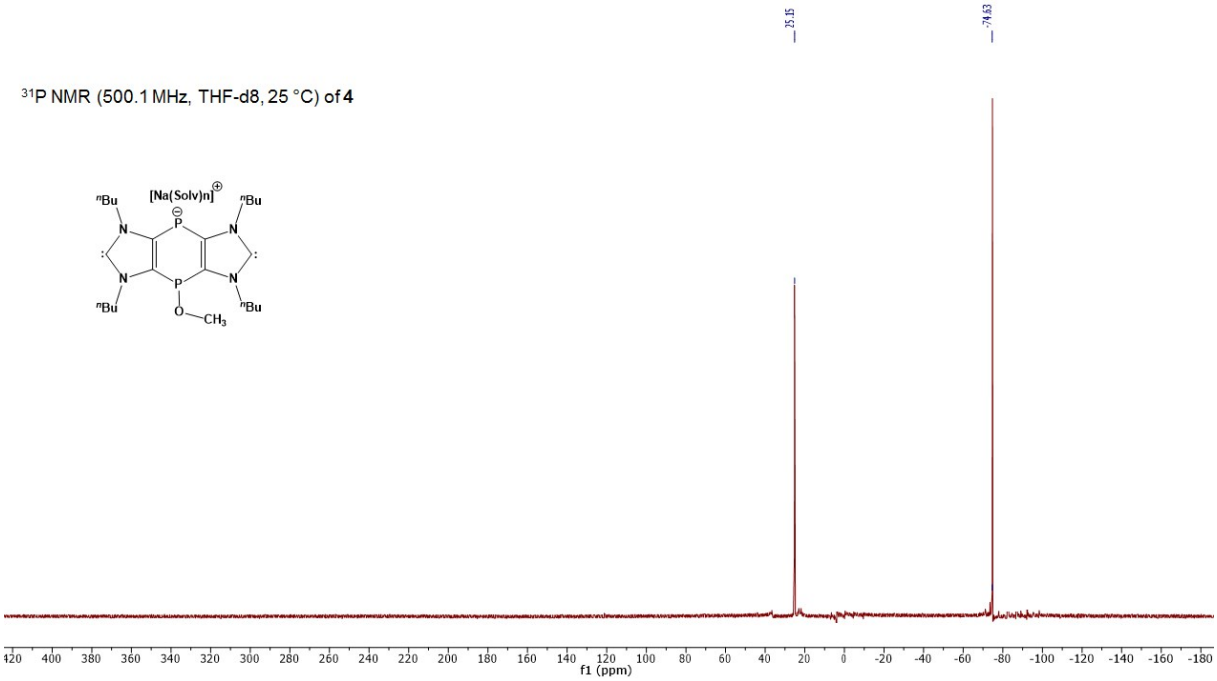

Figure S12: ^{31}P NMR spectrum of compound **4**

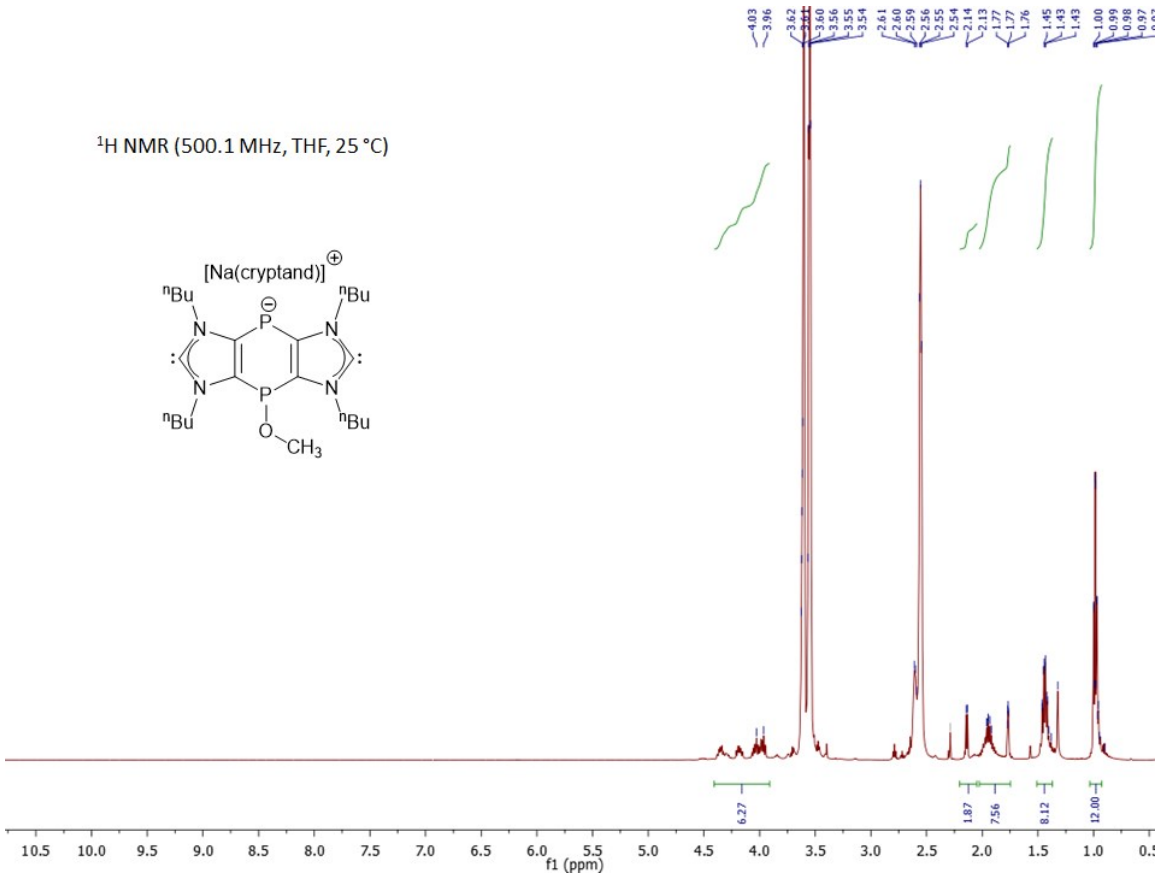

Figure S13: ^{1}H NMR spectrum of compound **4**

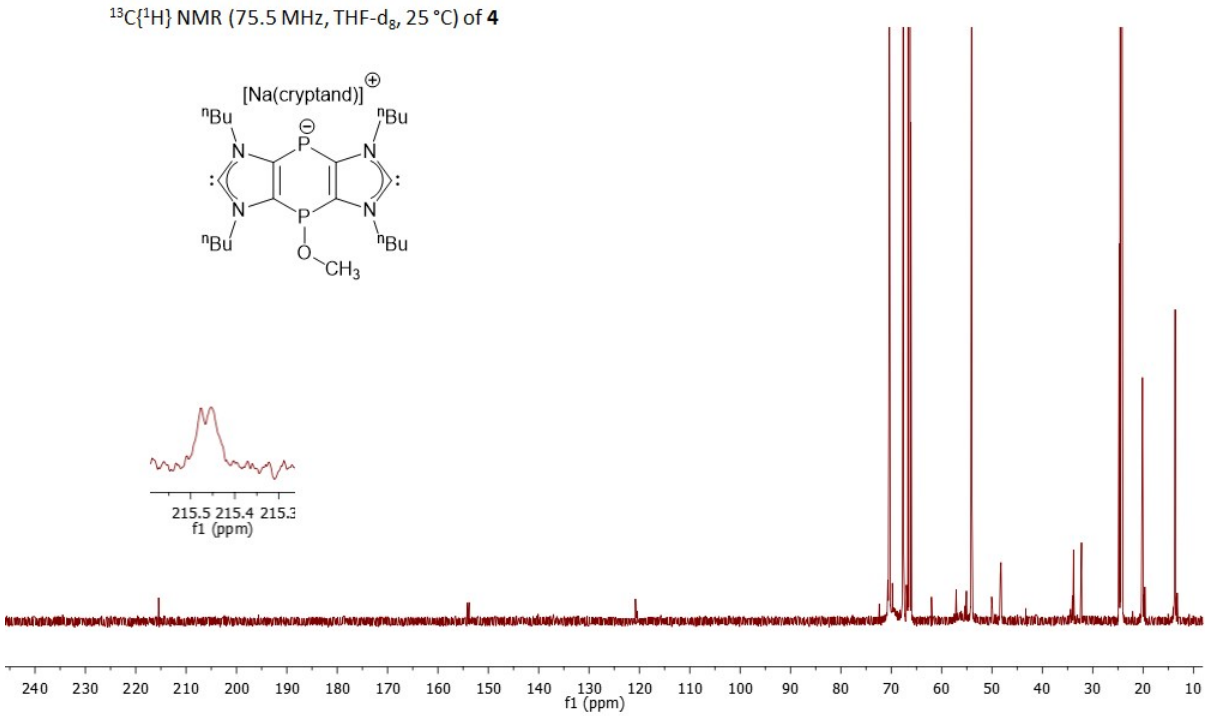

Figure S14: ^{13}C{^{1}H} NMR spectrum of compound **4**

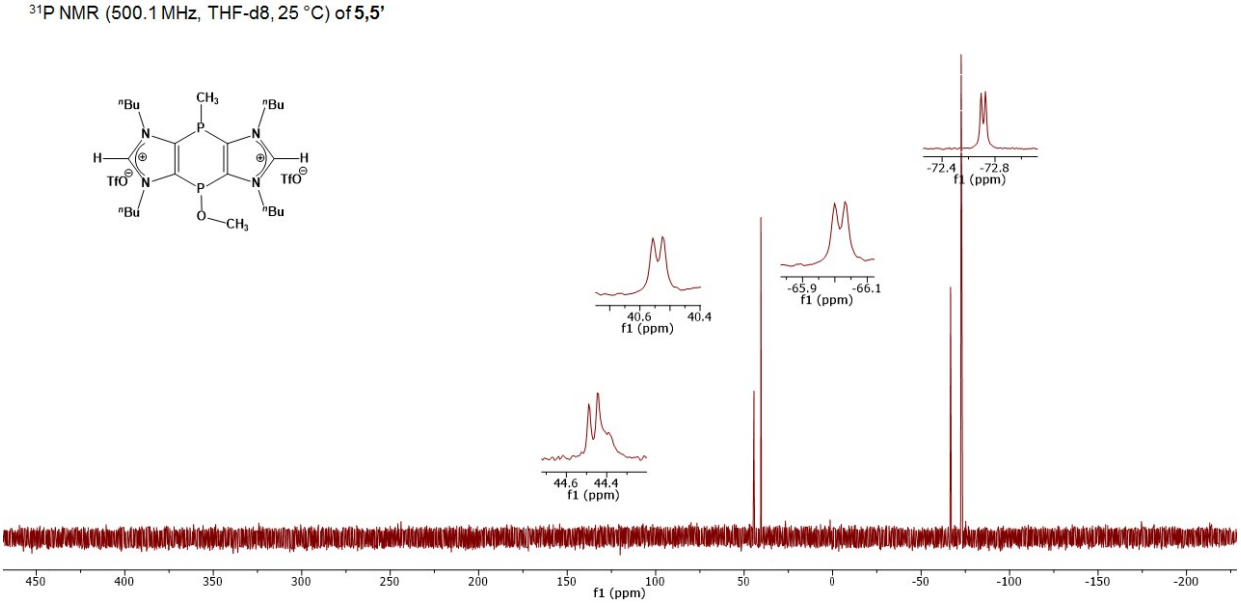

Figure S15: ^{31}P NMR spectrum of compound **5**$^{cis/trans}$

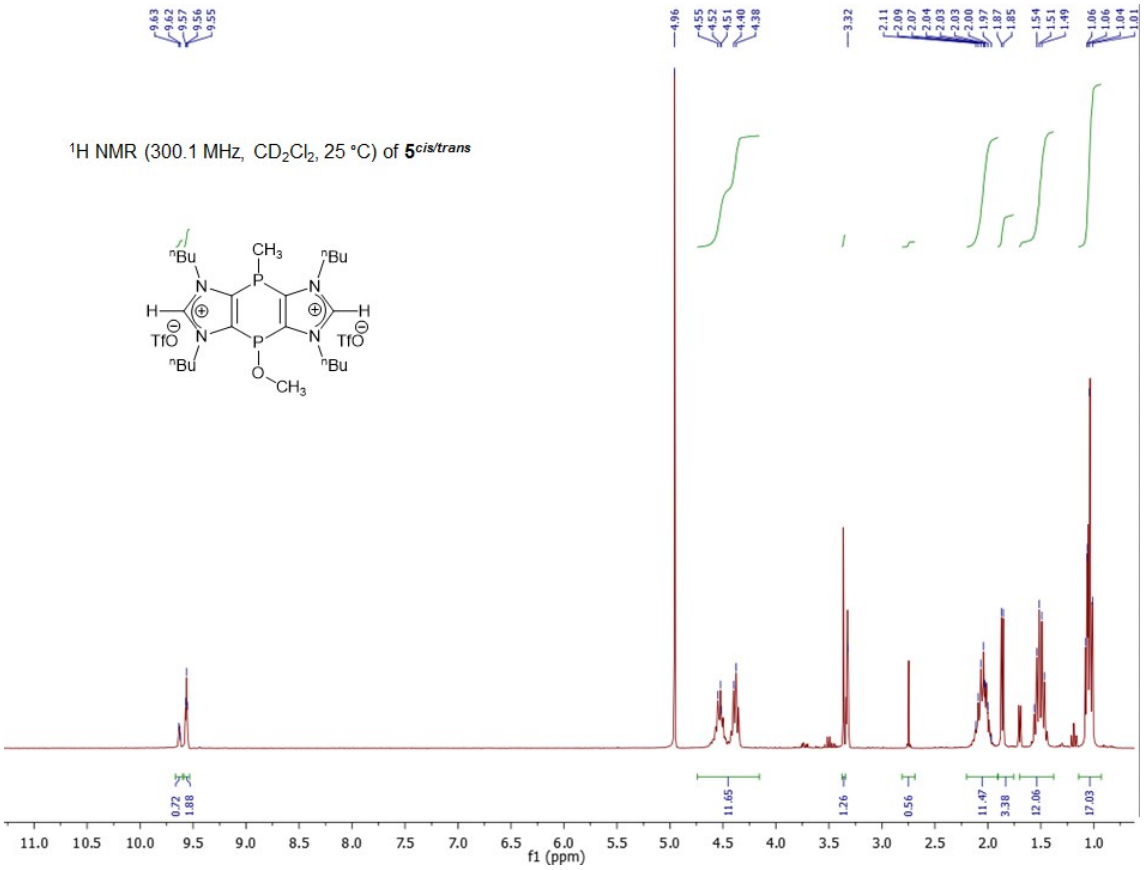

Figure S16: ^{1}H NMR spectrum of compound **5**$^{cis/trans}$

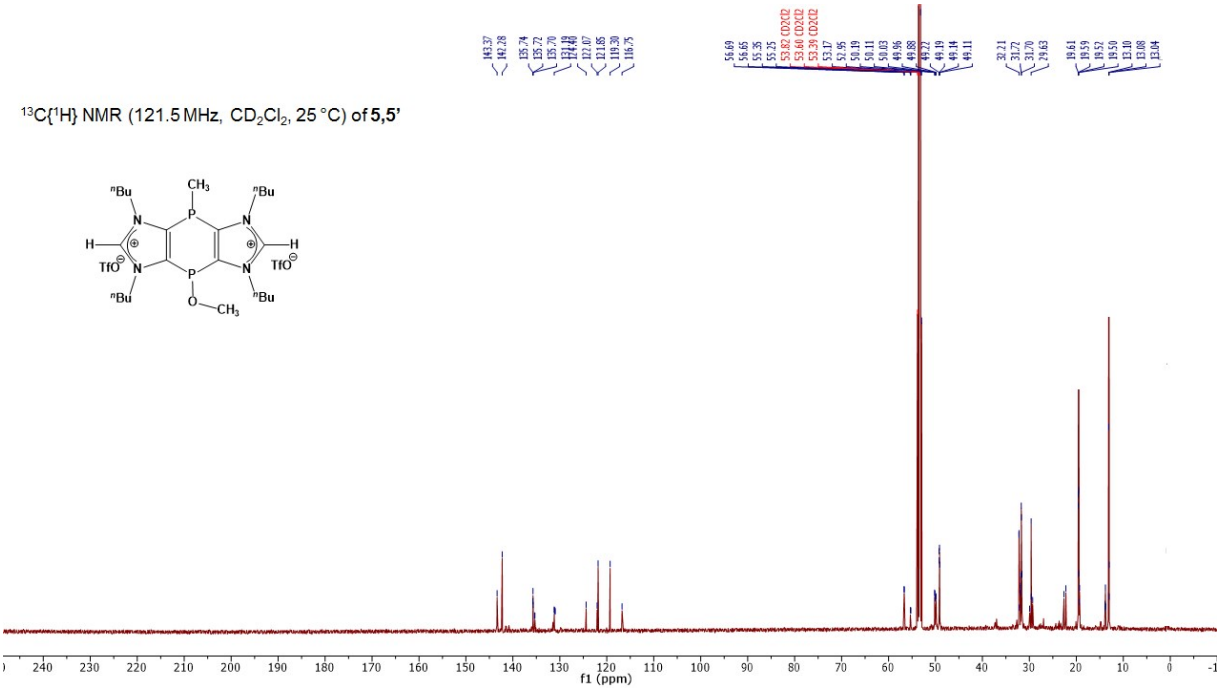

Figure S17: $^{13}C\{^{1}H\}$ NMR spectrum of compound **5**$^{cis/trans}$

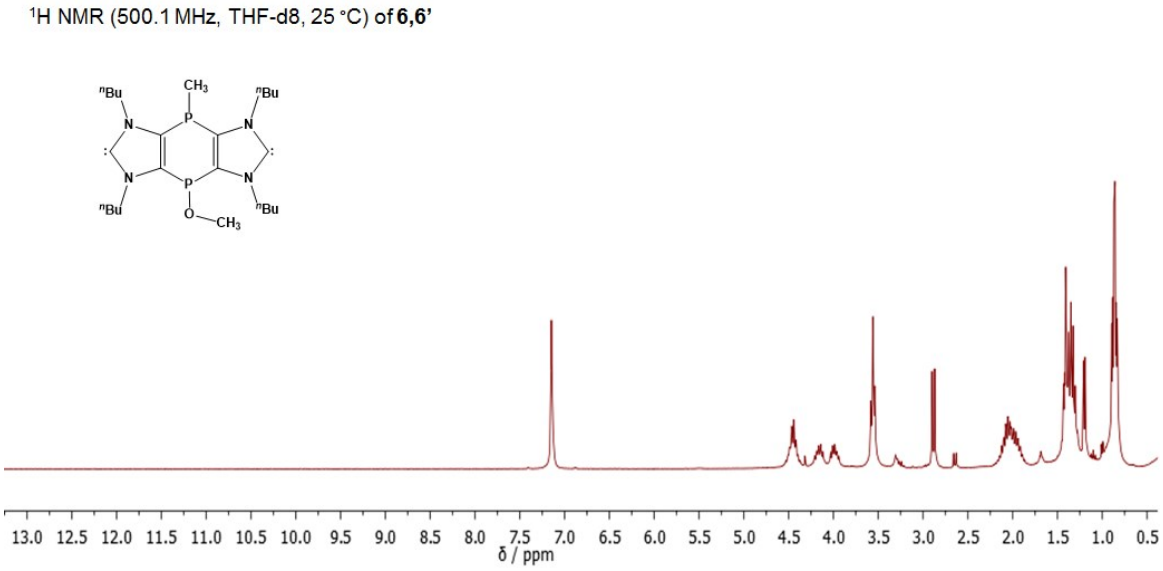

Figure S18: ^{1}H NMR spectrum of compound **6**$^{cis/trans}$

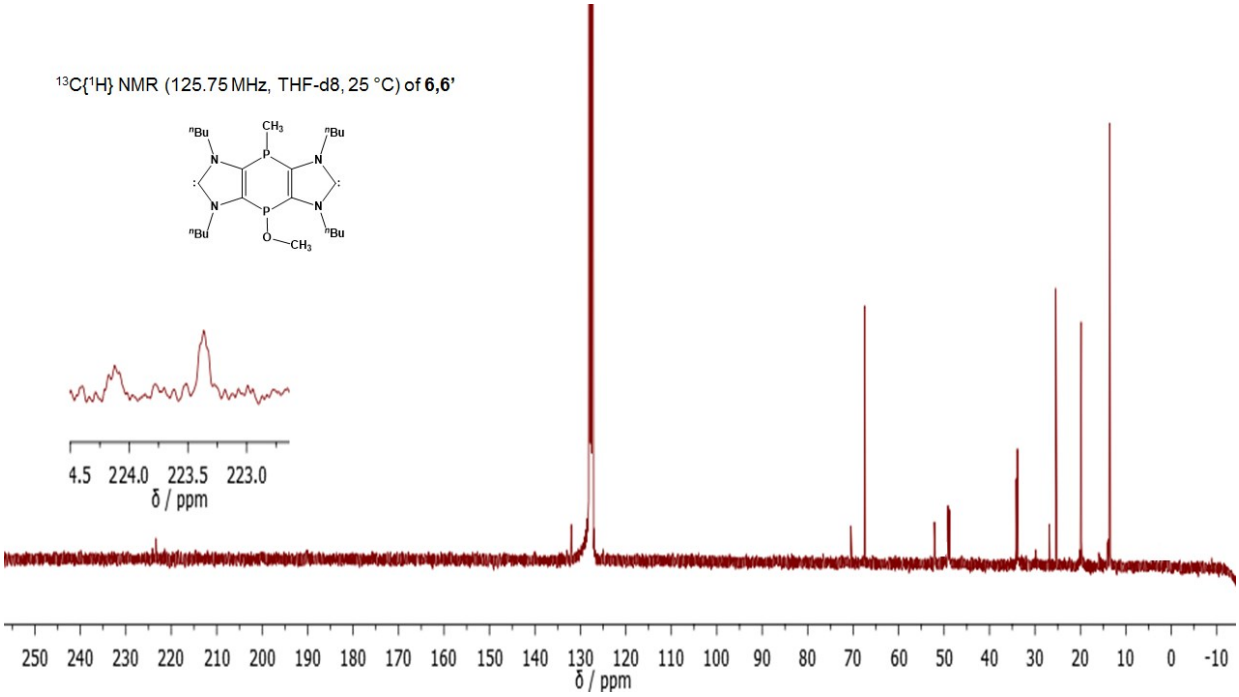

Figure S19: ^{1}H NMR spectrum of compound **6**$^{cis/trans}$

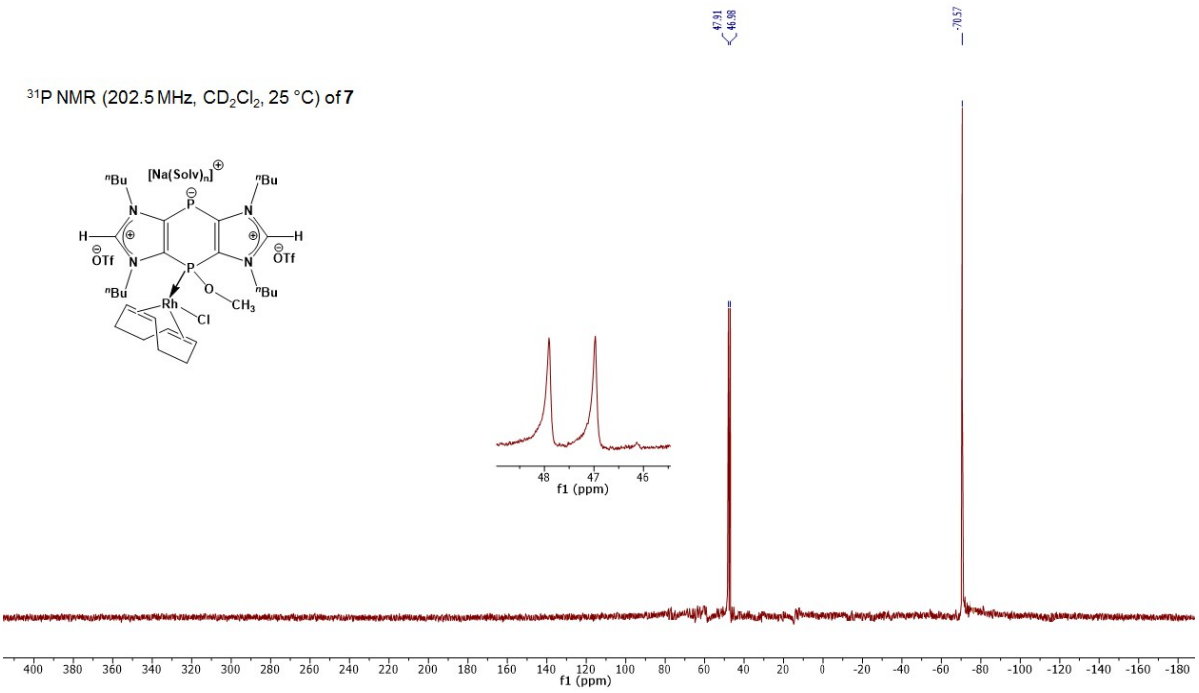

Figure S20: ^{31}P NMR spectrum of compound **7**

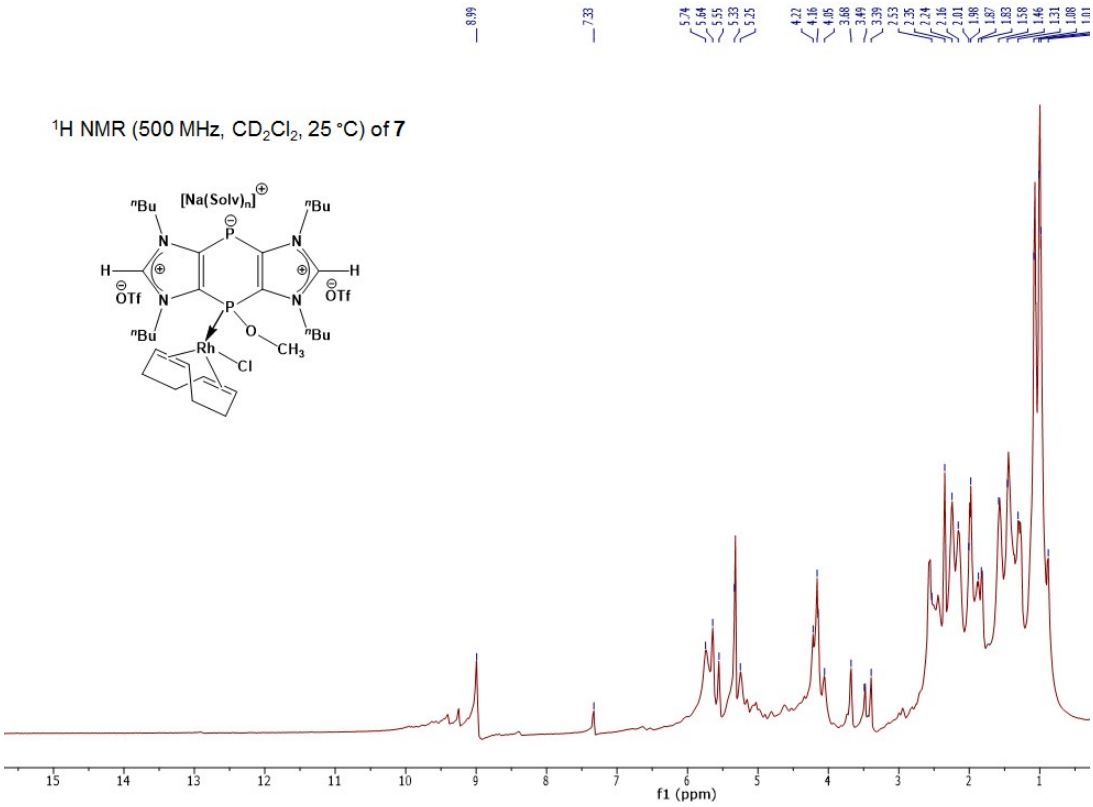

Figure S21: ^{1}H NMR spectrum of compound **7**

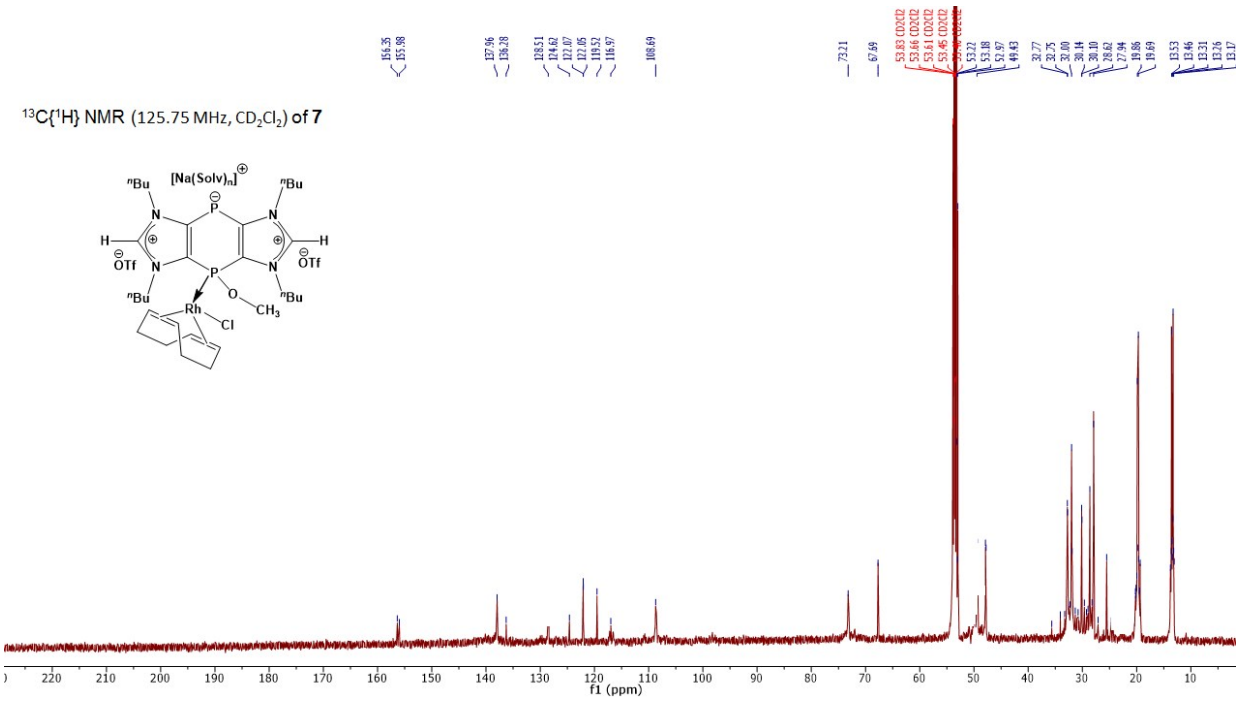

Figure S22: $^{13}C\{^1H\}$ NMR spectrum of compound **7**

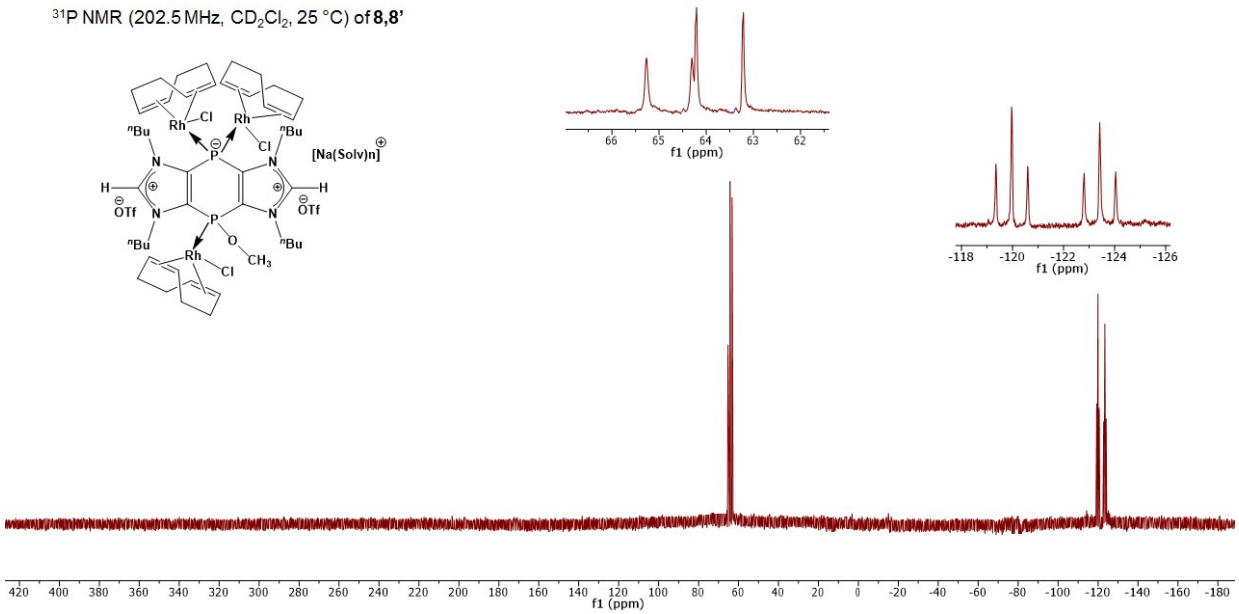

Figure S23: ^{31}P NMR spectrum of compound **8***cis/trans*

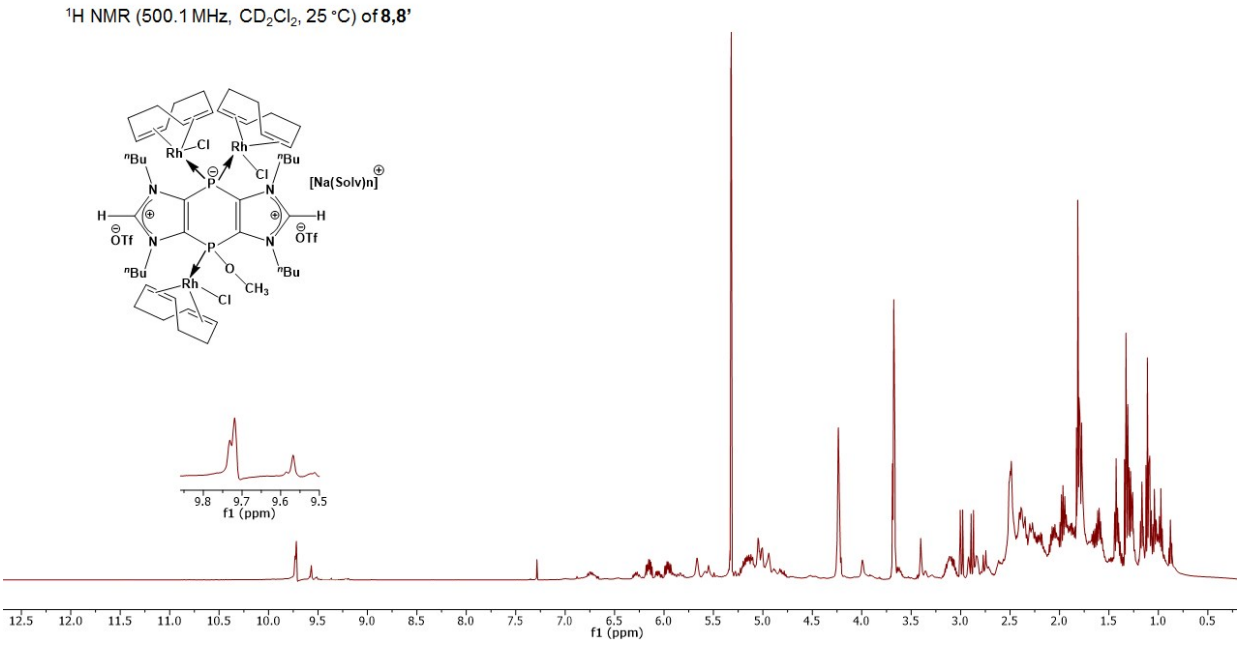

Figure S24: ^{1}H NMR spectrum of compound **8***cis/trans*

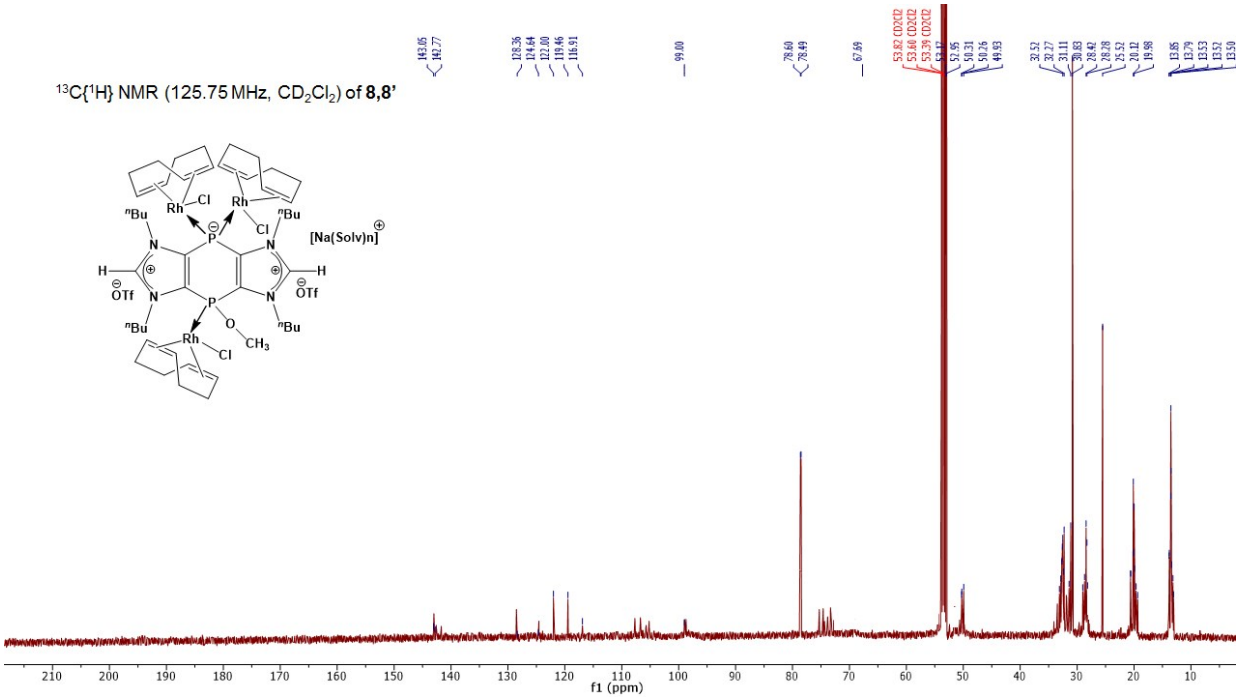

Figure S25: $^{13}C\{^{1}H\}$ NMR spectrum of compound **8***cis/trans*

2. UV-vis spectroscopic analysis

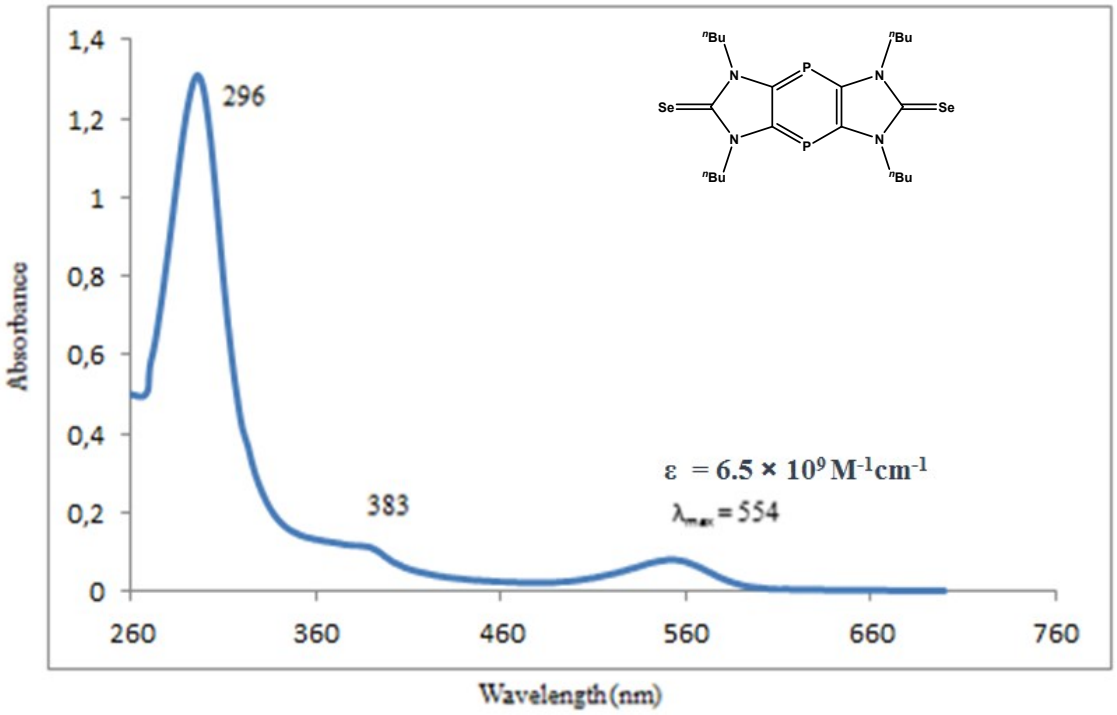

Figure S26. The UV spectrum of **1** ($2x10^{-7}$ mM) in CH_2Cl_2

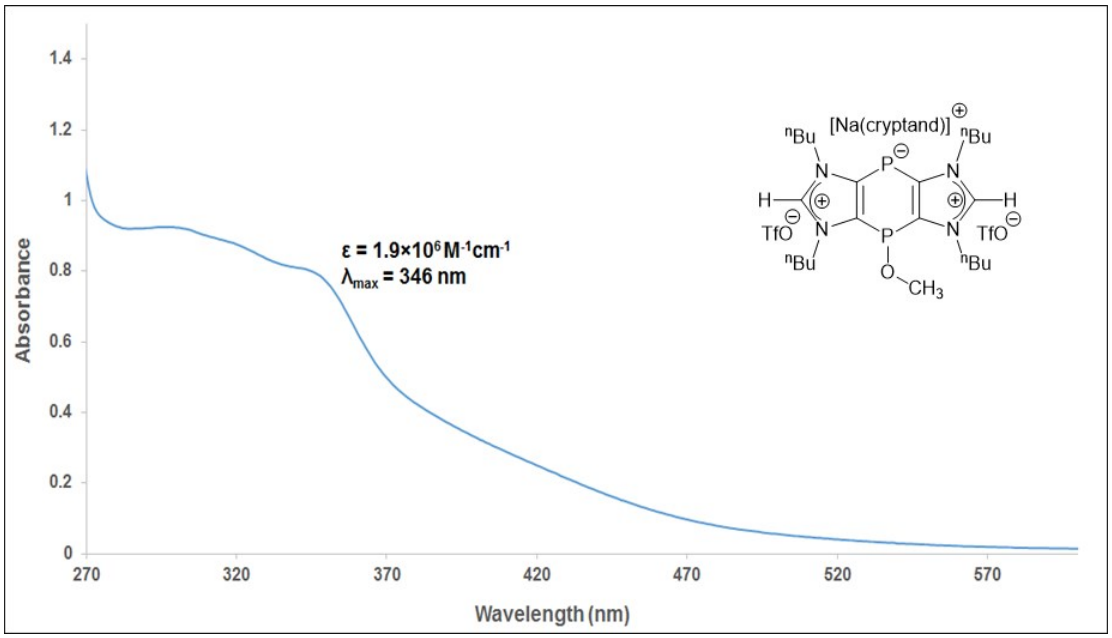

Figure S27. The UV spectrum of **3** in CH_2Cl_2

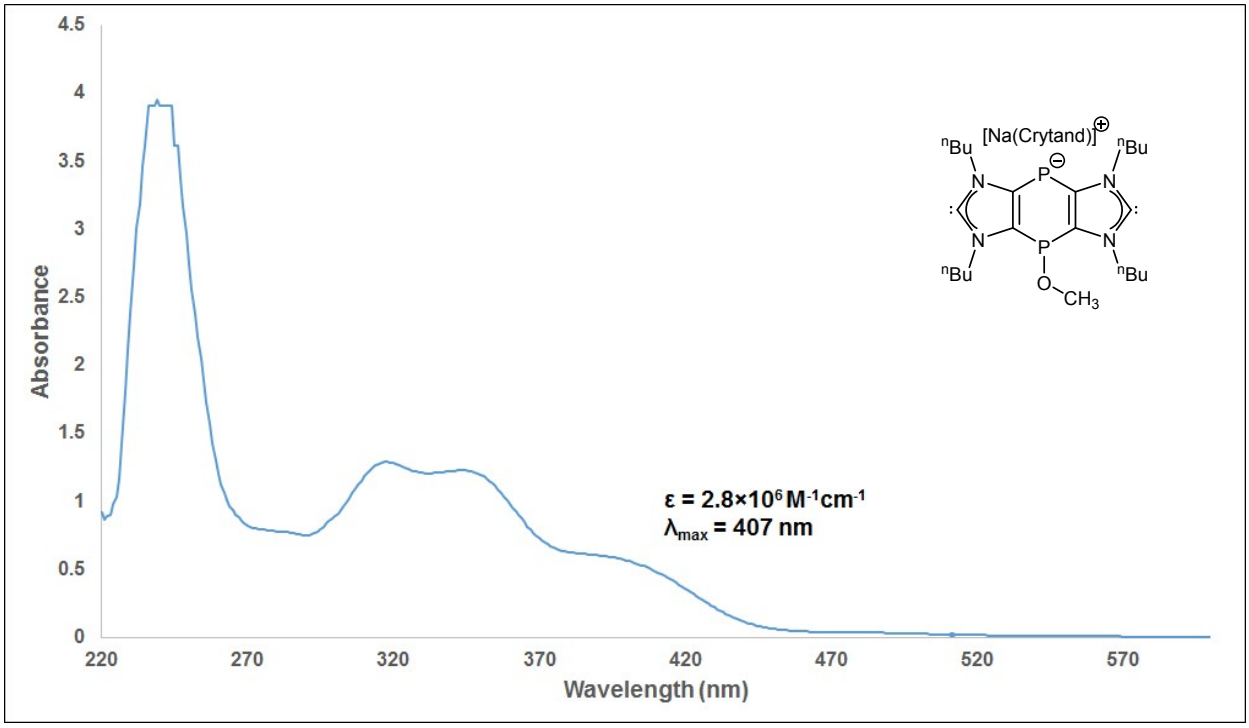

Figure S28. The UV spectrum of **4** in THF

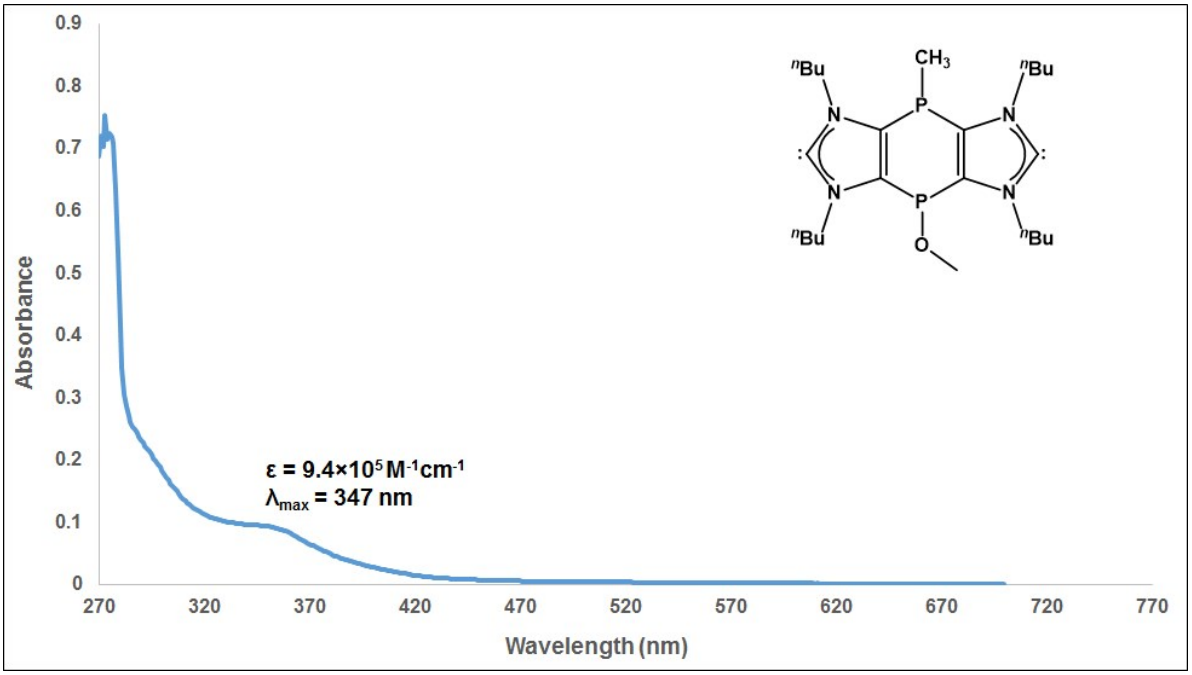

Figure S29. The UV spectrum of **6**$^{cis/trans}$ in THF

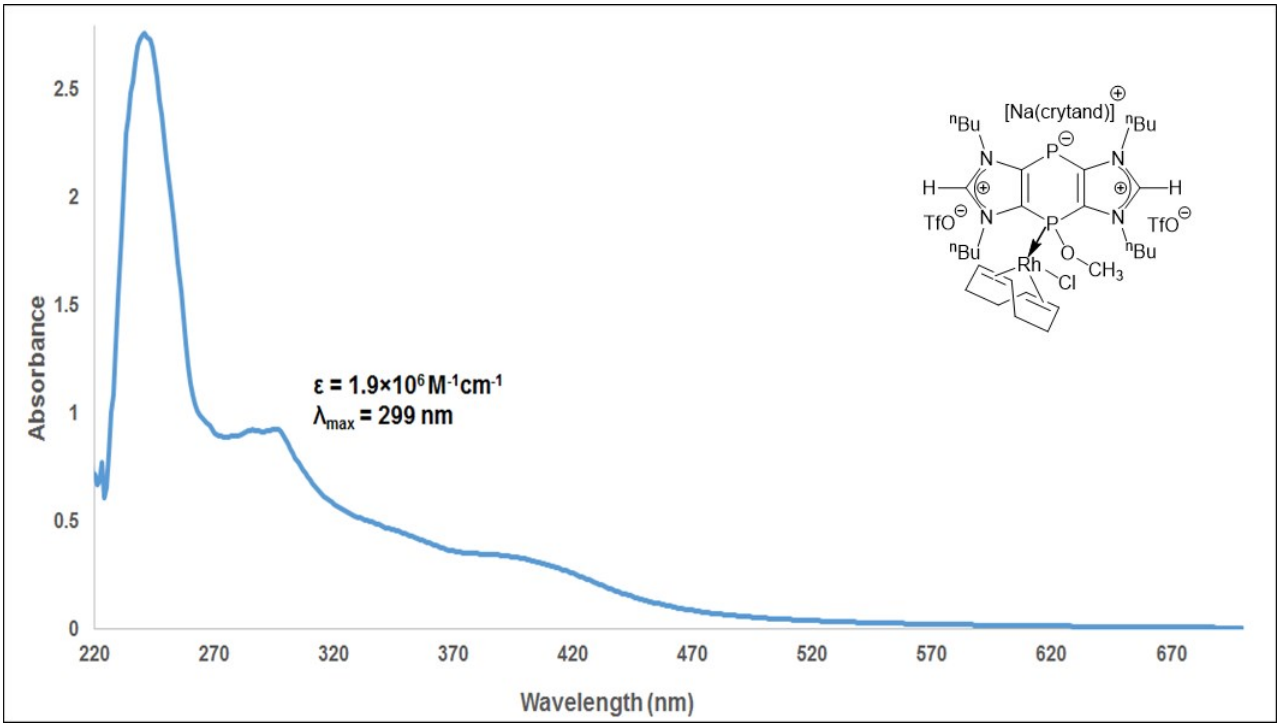

Figure S30. The UV spectrum of **7** in CH_2Cl_2

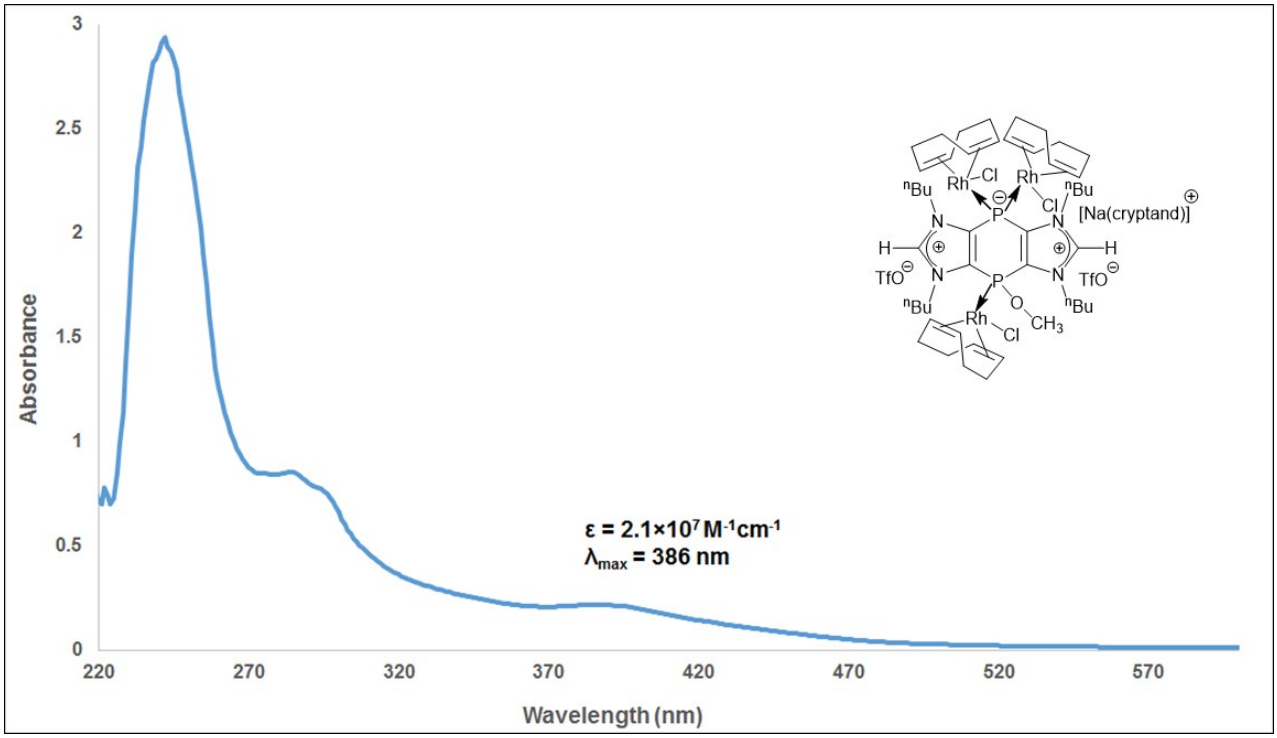

Figure S31. The UV spectrum of **8**$^{cis/trans}$ in CH_2Cl_2

3. X-ray diffraction studies

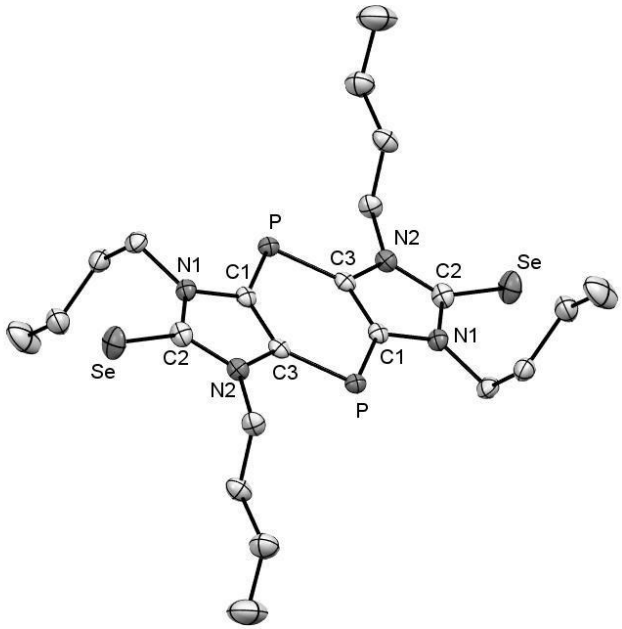

Figure S32: Molecular structure of **1**. Ellipsoids are set at 50 % probability and hydrogen atoms are omitted for clarity. Selected bond lengths [Å] and angles [°]: Se-C2 1.829(2), N1–C2 1.366(3), C1-C3 1.408(3), C1-P 1.744(2), C1-P-C3 96.92(10), N1-C2-N2 106.2(18).

Crystal Data for 1: Suitable single-crystals of **1** were obtained from a concentrated methylene chloride and diethyl ether mixture solution (1:0.3) at -4 °C. Data were collected with a with a Bruker X8-KappaApexII diffractometer equipped with a low-temperature device at 100 K by using graphite monochromated Mo Kα radiation (λ = 0.71073 Å). The structure was solved by Patterson methods (SHELXS-97)[1] and refined by full-matrix least-squares on F^2 (SHELXL-97).[1] $C_{22}H_{36}N_4P_2Se_2$, M = 576.41, crystal dimensions 0.3 × 0.1 × 0.06 mm^3, monoclinic, space group P21/n, Z = 4, a = 9.5787(5) Å, b = 24.9549(12) Å, c = 12.3331(6) Å, α = 90 °, β = 96.935(2)°, γ = 90°, V = 2926.5(3) $Å^3$, d_c = 1.308 g cm^{-3}, μ = 2.651 mm^{-1}, T = 100 K, transmission factors (min./max.) 0.4726/0.7460, empirical absorption correction, 2θmax= 56°, no. of unique data 7062, Rint = 0.0582, R1 (for I > 2σ(I)) = 0.0314, wR2 (for all data) = 0.0707, final R, R_1 = 0.0472, wR_2 = 0.0758, goodness of fit 1.014, F(max./min.) = 0.54/-0.40 e $Å^{-3}$.

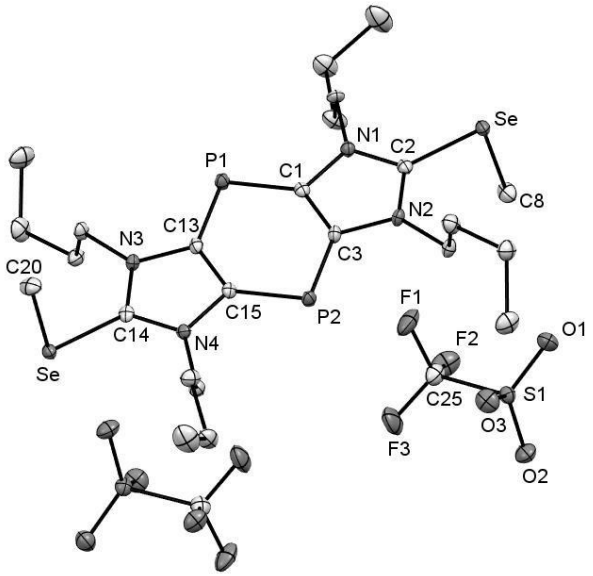

Figure S33: Molecular structure of **2** (two TfO anions) Ellipsoids are set at 50 % probability and hydrogen atoms are omitted for clarity. Selected bond lengths [Å] and angles [°]:C2–Se1 1.896(4), Se1–C8 1.952(4), C2–N2 1.339(5), N2–C3 1.397(5), C3–P2 1.736(4), C1–C3 1.412(6); N1–C2-N2 108.8(3), C3–P2–C15 96.3(2).

Crystal Data for 2: Suitable single-crystals of **2** were obtained from a concentrated mixture of dichloromethane and diethylether solution (1: 0.2) at -4 °C. Data were collected with a with a Bruker X8-KappaApexII diffractometer equipped with a low-temperature device at 100 K by using graphite monochromated Cu Kα radiation (λ = 0.71073Å). The structure was solved by Patterson methods (SHELXS-97)[1] and refined by full-matrix least-squares on F^2 (SHELXL-97).[1] $C_{26}H_{42}F_6N_4O_6P_2S_2Se_2$= 904.61, crystal dimensions 0.16 × 0.14 × 0.09 mm^3 orthorhombic, space group Pca21, Z = 4, a = 16.4677(7) Å, b = 9.3211(4) Å, c = 23.9930(9) Å, α = 90 °, β = 90 °, γ = 90 °, V = 3682.9(3) $Å^3$, d_c = 1.632 g cm^{-3}, μ = 2.282 mm^{-1}, T = 100 K, transmission factors (min./max.) 0.5453/0.7461, empirical absorption correction, 2θmax= 56°, no. of unique data 8876, Rint = 0.0507, R1 (for I > 2σ(I)) = 0.0298, wR2 (for all data) = 0.0632, goodness of fit 1.028, F(max./min.) = 0.59/-0.33 e $Å^{-3}$. Refined as an inversion twin, BASF = 0.489(8).

4. DFT calculations

All calculations were carried out with the Gaussian 09 program package.[1] Full geometry optimization calculations were performed, followed by calculation of the second derivatives at the optimized structures to establish the nature of the stationary points obtained. The Gibbs free energies were calculated based on the harmonic vibrational frequencies (atmospheric pressure, 298.15 K). All of the tricyclic compounds were calculated with methyl substituents at the nitrogen atoms (instead of *n*-butyl) to reduce the computational time and they were labelled by the special character ‘, and for the salts counterions were not included in the calculations, since it is most likely, that under the experimental conditions no contact ion pairs were formed in the solution. Kohn-Sahm orbitals were calculated at B3LYP/6-31+G*//M06-2X/6-31+G* for better comparisons with the former works. For the TD DFT calculated excited states only the five lowest energy excitations were listed. In order to establish the stability of the carbenes the following isodesmic reaction was used:

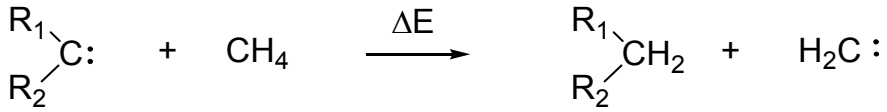

We have shown[2] that the stabilization energy of this reaction is in an excellent linear correlation with the decreasing dimerization energy of the carbenes, providing an easy way to assess the stability of carbenes. The highest reported stabilization energy was obtained for imidazolium-2-ylidene based NHC’s (111-113 kcal/mol).[3] Since the stabilization energies obtained for **4’** (113.3 kcal/mol) and **6’**$^{cis/trans}$ (108.8/108.6 kcal/mol) are close to these values, we can establish that the carbene stability is only slightly affected either in the anionic or in the neutral tricyclic bis-carbenes.

compound 1′

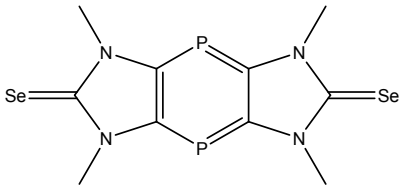

ΔE(singlet-triplet)= -43.5 kcal/mol (at M06-2X/6-311+G** level of theory)

	middle ring	outer ring
NICS(0)	-8.1	-7.8

NICS(1)	-9.8	-7.4

TD-DFT results at B3LYP/6-311+G**//M06-2X/6-311+G** level of theory (first 5 excited state):
The position of the intense (f: 0.4281) HOMO-LUMO transition is matching favourably with the observed intense 554 nm band maximum. Similar excellent agreement was obtained for the the related tricyclic thiones (see refs 13 and 16 of the main body of the article)

excited state	wavelength	oscillator strength	transitions	contribution
1	569 nm	0.0000	HOMO-1-LUMO	0.70495
2	559 nm	0.4281	HOMO-LUMO	0.70415
3	557 nm	0.0001	HOMO-2-LUMO	0.70478
4	445 nm	0.0000	HOMO-3-LUMO	0.70169
			HOMO-4-LUMO	0.63968
5	361 nm	0.0637	HOMO-LUMO+1	0.28152

compound 2′ (calculated without OTf- counterions)

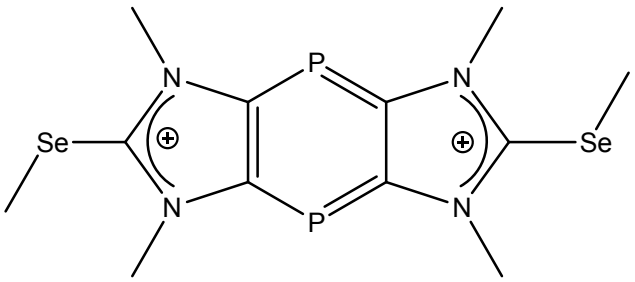

ΔE(singlet-triplet)= -38.1 kcal/mol (at M06-2X/6-311+G** level of theory)

	middle ring	outer ring
NICS(0)	-10.0	-10.9
NICS(1)	-11.5	-9.7 (-9.8)

TD-DFT results at B3LYP/6-311+G**//M06-2X/6-311+G** level of theory (first 5 excited state):

excited state	wavelength	oscillator strength	transitions	contribution
1	449 nm	0.2426	HOMO-LUMO	0.70225

2	422 nm	0.0004	HOMO-2-LUMO	0.27397
			HOMO-1-LUMO	0.64924
			HOMO-8-LUMO	-0.10058
3	367 nm	0.1189	HOMO-2-LUMO	0.63470
			HOMO-1-LUMO	-0.26708
			HOMO-3-LUMO	0.65888
4	310 nm	0.0564	HOMO-2-LUMO+1	0.11790
			HOMO-2-LUMO+2	-0.18501
			HOMO-2-LUMO+3	0.14838
5	279 nm	0.0001	HOMO-1-LUMO+3	0.34201
			HOMO-LUMO+1	0.53333
			HOMO-LUMO+2	0.22961

compound 3′ (calculated without Na+(cryptand) counterion)

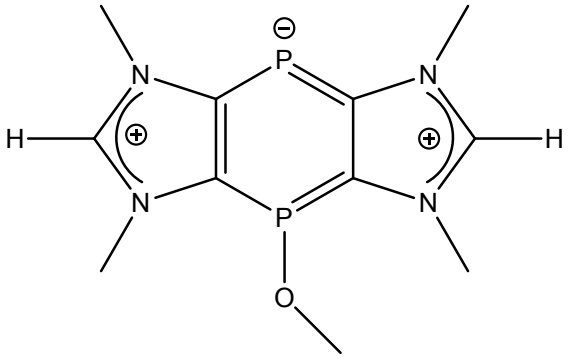

ΔE(singlet-triplet)= -59.3 kcal/mol (at M06-2X/6-311+G** level of theory)

	middle ring	outer ring
NICS(0)	-4.9	-11.1
NICS(1)	-3.7 (-6.9)	-9.0 (-8.6)

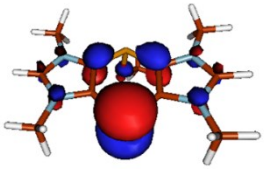

HOMO
ε=-7.80 eV

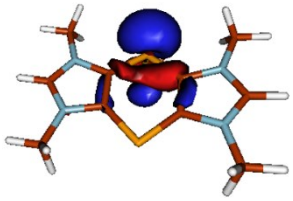

HOMO-1
ε=-9.70 eV

Kohn-Sahm HOMO and HOMO-1 at B3LYP/6-311+G**//M06-2X/6-311+G** level of theory

TD-DFT results at B3LYP/6-311+G**//M06-2X/6-311+G** level of theory (first 5 excited state):

excited state	wavelength	oscillator strength	transitions	contribution
1	427 nm	0.0468	HOMO-LUMO	0.69980
2	373 nm	0.0512	HOMO-LUMO+1	0.70406
3	315 nm	0.1213	HOMO-	0.68405

			LUMO+2	
			HOMO-LUMO+3	-0.11254
			HOMO-LUMO+3	0.23679
4	294 nm	0.0177	HOMO-LUMO+4	0.64304
			HOMO-LUMO+8	0.12298
			HOMO-LUMO+3	0.52503
			HOMO-LUMO+4	-0.22488
5	291 nm	0.0732		
			HOMO-LUMO+5	0.35487
			HOMO-LUMO+9	0.10730

compound 4′ (calculated without Na+(cryptand) counterion)

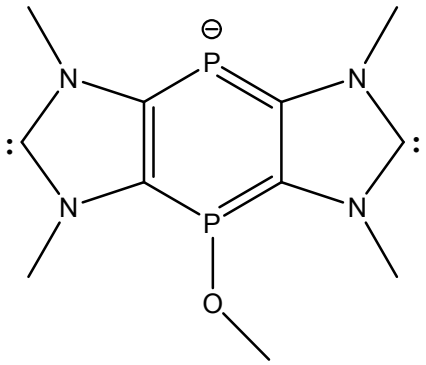

ΔE(singlet-triplet)= -58.0 kcal/mol (at M06-2X/6-311+G** level of theory)

	middle ring	outer ring
NICS(0)	-5.5	-9.0

NICS(1)	-4.0 (-7.0)	-9.1 (-8.8)

TD-DFT results at B3LYP/6-311+G**//M06-2X/6-311+G** level of theory (first 5 excited state):

excited state	wavelength	oscillator strength	transitions	contribution
1	427 nm	0.0027	HOMO-LUMO	0.69730
			HOMO-LUMO	-0.10153
2	403 nm	0.0299	HOMO-LUMO+1	0.56519
			HOMO-LUMO+2	-0.36770
			HOMO-LUMO+3	0.16108
3	392 nm	0.0702	HOMO-LUMO+1	0.40116
			HOMO-LUMO+2	0.48487
			HOMO-LUMO+3	-0.30430
4	384 nm	0.0228	HOMO-LUMO+2	0.32304
			HOMO-LUMO+3	0.59646
			HOMO-LUMO+4	-0.17882
5	380 nm	0.0029	HOMO-LUMO+2	0.10620
			HOMO-LUMO+3	0.14828
			HOMO-LUMO+4	0.67930

compound 5' isomer cis

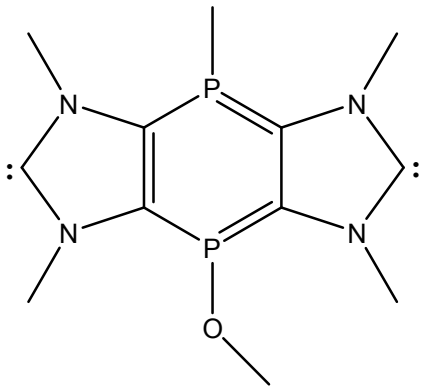

ΔE(singlet-triplet)= -63.7 kcal/mol

	middle ring	outer ring
NICS(0)	-0.1	-9.7
NICS(1)	-2.8 (0.4)	-9.6 (-10.0)

TD-DFT results at B3LYP/6-311+G**//M06-2X/6-311+G** level of theory (first 5 excited state):

excited state	wavelength	oscillator strength	transitions	contribution
1	338 nm	0.0000	HOMO-LUMO	0.70140
2	314 nm	0.0063	HOMO-1-LUMO	0.68940
3	299 nm	0.0235	HOMO-3-LUMO	-0.10651
			HOMO-2-LUMO	0.68536
4	287 nm	0.0870	HOMO-4-LUMO	0.23726
			HOMO-3-LUMO	0.64308
5	272 nm	0.0401	HOMO-4-LUMO	0.65283
			HOMO-3-LUMO	-0.21402
			HOMO-2-LUMO	-0.12004

compound 5' isomer trans

	middle ring	outer ring

NICS(0)	-1.9	-9.9
NICS(1)	-2.4 (-2.1)	-9.8 (-10.0)

TD-DFT results at B3LYP/6-311+G**//M06-2X/6-311+G** level of theory (first 5 excited state):

excited state	wavelength	oscillator strength	transitions	contribution
1	309 nm	0.0057	HOMO-LUMO	0.69816
2	288 nm	0.0343	HOMO-2-LUMO	0.53687
			HOMO-1-LUMO	0.42419
			HOMO-LUMO+2	-015339
3	281 nm	0.1923	HOMO-3-LUMO+2	0.11341
			HOMO-2-LUMO	-0.42496
			HOMO-1-LUMO	0.54208
4	276 nm	0.0138	HOMO-3-LUMO	0.69994
5	248 nm	0.0009	HOMO-2-LUMO	0.15461
			HOMO-LUMO+2	0.68254

Possible isomers of **7'** and their relative energies at M06-2X/6-311+G** level of theory:

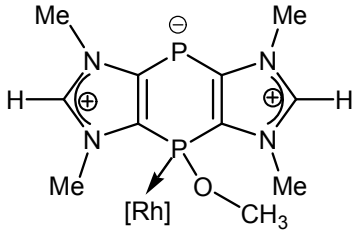

0.0 kcal/mol

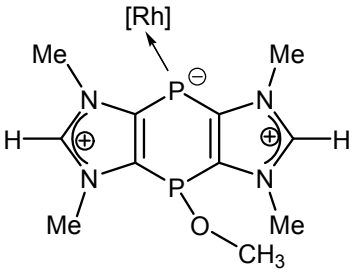

cis: 5.2 kcal/mol
trans: 5.8 kcal/mol

XYZ geometries and total energies of the investigated systems

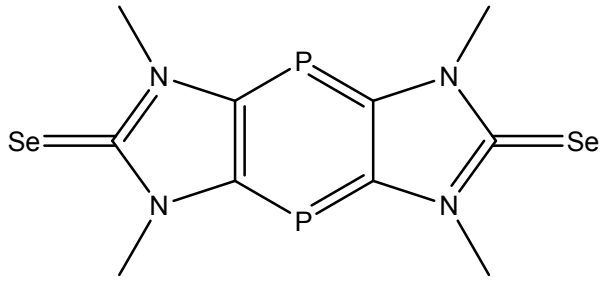

E(M06-2X/6-311+G**) = -6093.038121

C	-0.004396	0.031982	-0.010249
N	0.004730	0.024227	1.357630
C	1.300241	0.014321	1.849872
C	2.145694	0.016038	0.724122
N	1.311819	0.026945	-0.382805
P	1.663366	0.002510	3.556260
C	3.403367	-0.006379	3.429380
C	4.248827	-0.004285	2.303640
N	5.544337	-0.014113	2.795885
C	5.553445	-0.022077	4.163766
N	4.237223	-0.017324	4.536313
P	3.885688	0.007438	0.597251
C	3.752785	-0.022515	5.904635
C	-1.174323	0.025880	2.204304
C	1.796232	0.031475	-1.751139
C	6.723410	-0.015313	1.949243
Se	7.008822	-0.036071	5.256776
Se	-1.459779	0.046137	-1.103248
H	4.615474	-0.032268	6.566293
H	3.153926	0.872402	6.085318
H	3.142159	-0.911613	6.074270
H	7.599324	-0.024282	2.593302
H	6.718074	-0.903334	1.314002
H	6.728040	0.880690	1.325300
H	0.933527	0.039821	-2.412794
H	2.405961	0.921034	-1.921611
H	2.395984	-0.863003	-1.930996
H	-1.168752	0.914067	2.839320
H	-2.050239	0.034883	1.560251

H -1.179123 -0.869957 2.828479

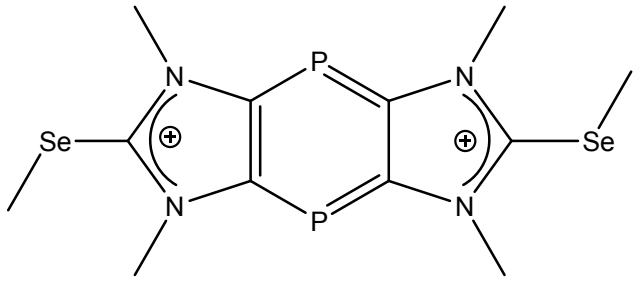

E(M06-2X/6-311+G**) = -6172.267290

C 0.016555 -0.199909 -0.021277
N 0.012942 -0.154655 1.320674
C 1.324379 -0.097405 1.790952
C 2.149929 -0.087364 0.648070
N 1.290358 -0.174875 -0.447294
P 1.700349 -0.062806 3.494611
C 3.434499 0.019461 3.318834
C 4.260115 0.067281 2.176949
N 5.567621 0.170359 2.652528
C 5.562806 0.150574 3.995760
N 4.291401 0.060699 4.418081
P 3.883361 0.013736 0.473870
C 3.831552 0.013847 5.811224
C -1.165999 -0.165482 2.195039
C 1.731679 -0.297652 -1.839702
C 6.747542 0.350234 1.801595
Se 7.063723 0.307675 5.141377
C 8.149380 -1.158363 4.407830
Se -1.538367 -0.359132 -1.092198
C -1.219032 1.156983 -2.302766
H 4.680498 -0.202722 6.454546
H 3.391733 0.973238 6.084958
H 3.093246 -0.781791 5.908586
H 7.513372 0.866298 2.377247
H 7.113333 -0.615267 1.450976
H 6.470710 0.973610 0.952268
H 0.957100 -0.813712 -2.403536
H 1.926537 0.687579 -2.264298
H 2.639587 -0.899074 -1.863912

H	-1.045320	0.607816	2.953361
H	-2.048296	0.050797	1.598174
H	-1.265024	-1.144082	2.665506
H	8.867315	-1.369560	5.199318
H	7.523957	-2.031752	4.244334
H	8.673456	-0.848129	3.509105
H	-2.200641	1.357962	-2.730014
H	-0.889915	2.020187	-1.730714
H	-0.522201	0.890603	-3.091483

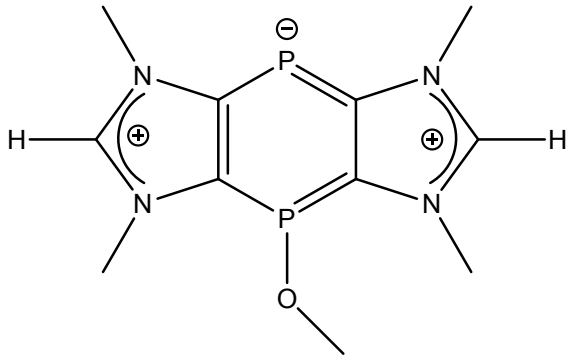

E(M06-2X/6-311+G**) = -1405.993350

N	-0.064387	-0.086160	-0.021611
C	-0.029126	-0.049292	1.372427
C	1.323217	-0.016281	1.710268
N	2.035586	-0.060794	0.505307
C	1.180920	-0.098608	-0.500346
P	-1.524109	-0.145294	2.329901
C	-0.652964	-0.326210	3.874117
C	0.690641	-0.281154	4.234017
N	0.750584	-0.545888	5.603900
C	-0.473889	-0.736121	6.059370
N	-1.340962	-0.612617	5.052914
C	1.968409	-0.554065	6.410575
P	2.144511	0.200287	3.300123
O	2.040258	1.840852	3.604620
C	3.112077	2.666110	3.163212
C	-2.787977	-0.766781	5.147536
C	3.490547	-0.090278	0.374540
C	-1.286946	-0.141520	-0.814244
H	3.745991	-0.134354	-0.682156

H	3.917629	0.809899	0.815787
H	3.881347	-0.968632	0.886017
H	-1.026026	-0.177054	-1.869839
H	-1.850070	-1.034016	-0.538609
H	-1.888103	0.744987	-0.611131
H	-3.054507	-0.996438	6.177016
H	-3.269085	0.161651	4.838964
H	-3.105236	-1.577433	4.490779
H	2.436039	0.429189	6.360282
H	1.705548	-0.785039	7.440683
H	2.651318	-1.310384	6.026431
H	3.038734	3.607823	3.703282
H	4.084420	2.205511	3.370733
H	3.025577	2.872181	2.091263
H	1.445257	-0.137586	-1.545274
H	-0.734321	-0.955653	7.082600

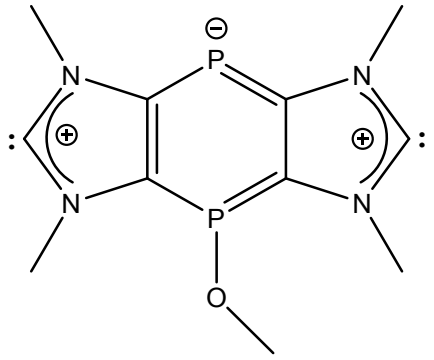

E(M06-2X/6-311+G**) = -1404.995104

C	0.021864	-0.216384	0.187004
N	0.083544	-0.288715	1.532977
C	1.379543	-0.082694	2.046170
C	2.186892	0.132264	0.944538
N	1.322779	0.043880	-0.148883
P	1.756923	0.011638	3.780953
O	1.463995	1.700794	4.001723
C	1.887402	2.225228	5.233275
P	3.943205	0.413400	0.764491
C	4.326169	0.152908	2.487696
C	3.528277	-0.094497	3.592689
N	4.428265	-0.336550	4.656864

C	5.725204	-0.248619	4.293690
N	5.635567	0.063830	2.964786
C	4.013305	-0.722364	5.986994
C	-1.070689	-0.529017	2.369102
C	1.771980	0.197263	-1.513086
C	6.789033	0.241214	2.113747
H	4.915106	-0.860384	6.580315
H	3.385046	0.048268	6.441996
H	3.441534	-1.653495	5.955114
H	7.677317	0.114588	2.729343
H	6.780557	-0.496547	1.306031
H	6.782076	1.238722	1.665168
H	0.905740	0.080158	-2.161140
H	2.217933	1.185382	-1.658518
H	2.527013	-0.557335	-1.751852
H	-1.213214	0.300799	3.067053
H	-1.935391	-0.617489	1.714399
H	-0.944704	-1.449493	2.945289
H	1.541430	3.258840	5.297912
H	1.471297	1.662990	6.083587
H	2.983249	2.219874	5.315958

E(M06-2X/6-31+G*)= -1404.7682402

N	-0.011816	-0.012641	-0.009248
C	-0.011067	-0.007753	1.387440
C	1.330649	0.003901	1.740924
N	2.039118	-0.017080	0.517260
C	1.237227	-0.030195	-0.571086
P	-1.509747	-0.117597	2.354139
C	-0.672524	-0.327150	3.922628
C	0.662538	-0.287606	4.288644
N	0.686839	-0.578083	5.666874
C	-0.538599	-0.793734	6.194643
N	-1.352191	-0.632701	5.103971
C	1.902922	-0.614693	6.446183
P	2.101760	0.166379	3.344241
O	2.065749	1.865822	3.661552
C	2.982430	2.627318	2.919035
C	-2.787333	-0.780777	5.161322
C	3.478908	-0.101882	0.425322

C	-1.228158	-0.039290	-0.786736
H	3.736279	-0.125608	-0.634395
H	3.957265	0.760961	0.902593
H	3.842973	-1.010062	0.918202
H	-0.948610	-0.046737	-1.840963
H	-1.814036	-0.933829	-0.544677
H	-1.841978	0.842018	-0.567326
H	-3.054927	-1.019461	6.191381
H	-3.280391	0.148078	4.851801
H	-3.115185	-1.583396	4.490436
H	2.419980	0.350147	6.392092
H	1.624418	-0.830413	7.478474
H	2.578203	-1.392655	6.073063
H	2.971611	3.647870	3.314676
H	4.008559	2.229692	2.999595
H	2.705792	2.663739	1.853714

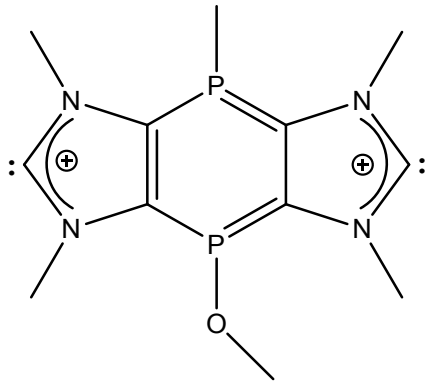

isomer cis: E(M06-2X/6-311+G**) = -1444.833724

C	0.106601	-0.362391	0.096504
N	0.166333	-0.301806	1.451970
C	1.451504	-0.073067	1.932548
C	2.250203	0.014279	0.829858
N	1.412273	-0.167567	-0.258024
P	1.852077	0.121660	3.683276
O	1.739359	1.797549	3.722219
C	2.063260	2.409685	4.960152
P	4.039269	0.326445	0.683628
C	4.458746	0.015318	2.428520
C	3.647752	-0.113248	3.519041
N	4.498182	-0.404472	4.584863

C	5.807231	-0.461935	4.224257
N	5.748707	-0.200214	2.884557
C	4.052741	-0.675257	5.942694
C	-1.005879	-0.449225	2.299239
C	1.853785	-0.161738	-1.642772
C	6.932024	-0.169897	2.040891
H	4.941462	-0.876401	6.535554
H	3.523690	0.185102	6.357385
H	3.390528	-1.542027	5.961546
H	7.784333	-0.400731	2.674869
H	6.850187	-0.910262	1.243589
H	7.065490	0.819623	1.598466
H	0.981473	-0.366694	-2.258190
H	2.267060	0.812514	-1.913036
H	2.611992	-0.929522	-1.804355
H	-1.150494	0.447509	2.904855
H	-1.860408	-0.590100	1.642317
H	-0.897415	-1.314113	2.955617
H	1.772659	3.456534	4.888937
H	1.521997	1.942223	5.791138
H	3.141196	2.351946	5.151768
C	4.006601	2.187641	0.711416
H	3.605797	2.549252	-0.237297
H	3.388440	2.543677	1.536442
H	5.027604	2.559405	0.816087

E(M06-2X/6-31+G*) = -1444.5954481

N	-0.011816	-0.012641	-0.009248
C	-0.011067	-0.007753	1.387440
C	1.330649	0.003901	1.740924
N	2.039118	-0.017080	0.517260
C	1.237227	-0.030195	-0.571086
P	-1.509747	-0.117597	2.354139
C	-0.672524	-0.327150	3.922628
C	0.662538	-0.287606	4.288644
N	0.686839	-0.578083	5.666874
C	-0.538599	-0.793734	6.194643
N	-1.352191	-0.632701	5.103971
C	1.902922	-0.614693	6.446183
P	2.101760	0.166379	3.344241

O	2.065749	1.865822	3.661552
C	2.982430	2.627318	2.919035
C	-2.787333	-0.780777	5.161322
C	3.478908	-0.101882	0.425322
C	-1.228158	-0.039290	-0.786736
H	3.736279	-0.125608	-0.634395
H	3.957265	0.760961	0.902593
H	3.842973	-1.010062	0.918202
H	-0.948610	-0.046737	-1.840963
H	-1.814036	-0.933829	-0.544677
H	-1.841978	0.842018	-0.567326
H	-3.054927	-1.019461	6.191381
H	-3.280391	0.148078	4.851801
H	-3.115185	-1.583396	4.490436
H	2.419980	0.350147	6.392092
H	1.624418	-0.830413	7.478474
H	2.578203	-1.392655	6.073063
H	2.971611	3.647870	3.314676
H	4.008559	2.229692	2.999595
H	2.705792	2.663739	1.853714

isomer trans: E(M06-2X/6-311+G**) = -1444.834217

C	0.153667	0.258723	0.198432
N	0.288549	0.126238	1.544423
C	1.611441	-0.007846	1.953248
C	2.357656	0.024960	0.810193
N	1.446799	0.184719	-0.227473
P	2.075596	-0.298111	3.677822
O	1.675196	1.178053	4.354996
C	0.889094	1.147748	5.540302
P	4.153893	-0.061619	0.551654
C	4.618857	-0.048799	2.307907
C	3.856084	-0.081009	3.440012
N	4.753095	-0.019356	4.501473
C	6.049977	0.066399	4.103751
N	5.935279	0.038309	2.745399
C	4.350970	0.050960	5.895432
C	-0.834342	0.219966	2.460983
C	1.813298	0.273727	-1.630605
C	7.087675	0.101594	1.862779

H	5.252533	-0.024187	6.498271
H	3.849092	0.999461	6.096522
H	3.678169	-0.775975	6.136720
H	7.963597	0.253994	2.488276
H	7.201426	-0.830063	1.304190
H	6.983846	0.931492	1.161694
H	0.903845	0.484350	-2.187602
H	2.536313	1.076696	-1.783969
H	2.240807	-0.668121	-1.981470
H	-0.781220	1.150390	3.029721
H	-1.743204	0.203733	1.864676
H	-0.831920	-0.628963	3.149471
H	-0.079113	0.667850	5.367237
H	1.403325	0.619535	6.349153
H	0.727794	2.183586	5.834805
C	4.331620	-1.880016	0.193561
H	3.919721	-2.091802	-0.794708
H	5.391524	-2.139983	0.179619
H	3.815418	-2.479419	0.943637

E(M06-2X/6-31+G*) = -1444.5959032

N	-0.000758	0.000320	-0.001101
C	-0.000750	0.003332	1.389061
C	1.317075	0.005712	1.757328
N	2.039549	-0.005456	0.568175
C	1.252614	0.001886	-0.542294
P	-1.521779	0.038182	2.383640
C	-1.901141	-1.787648	2.443346
P	2.107926	-0.101027	3.383683
O	2.863345	1.392091	3.455983
C	4.236158	1.387777	3.829905
C	3.488480	0.063317	0.502439
C	-1.201755	0.006120	-0.818187
C	0.612124	0.236915	4.348173
N	0.637145	0.454494	5.722295
C	-0.600278	0.609571	6.267454
N	-1.410005	0.462501	5.178168
C	-0.710683	0.236165	3.998217
C	1.857817	0.598139	6.495457
C	-2.857339	0.549078	5.266415

H	3.773512	-0.066361	-0.541155
H	3.838619	1.034854	0.863359
H	3.934672	-0.734085	1.106279
H	-0.884241	0.087261	-1.857162
H	-1.768633	-0.920707	-0.685595
H	-1.836336	0.857500	-0.556678
H	-3.102186	0.814649	6.294222
H	-3.235348	1.316306	4.584949
H	-3.321542	-0.411424	5.021687
H	2.385164	1.511555	6.205080
H	1.573150	0.655310	7.545621
H	2.510861	-0.267102	6.339089
H	4.378511	0.968218	4.833036
H	4.844726	0.815323	3.119617
H	4.562400	2.429072	3.825755
H	-2.708899	-1.966633	3.159421
H	-2.246224	-2.118364	1.459062
H	-1.020977	-2.366650	2.734509

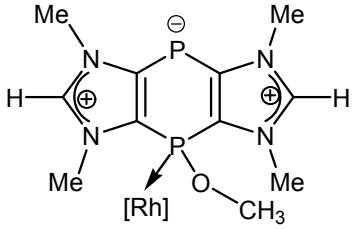

E(M06-2X/6-311+G**) = -2287.673345

N	-3.127299	-2.517559	-0.750522
C	-2.747038	-1.219543	-0.415185
C	-1.505696	-1.352900	0.194644
N	-1.191393	-2.711635	0.202195
C	-2.180915	-3.376116	-0.362730
P	-3.801428	0.164121	-0.816763
C	-2.683333	1.364616	-0.122281
N	-2.984217	2.725882	-0.190000
C	-1.996591	3.433324	0.359166
N	-1.051974	2.612381	0.781909
C	-1.441976	1.295327	0.506670
C	-4.198978	3.270976	-0.785177
P	-0.427055	-0.130211	0.932492

O	-0.709206	-0.465766	2.502298
C	0.017146	0.146922	3.577794
C	0.158843	3.034150	1.489773
C	0.015699	-3.313869	0.778657
C	-4.380704	-2.866908	-1.409112
Rh	1.708783	-0.113806	0.137002
C	1.365409	1.353987	-1.430784
C	2.638645	2.088223	-1.834367
C	3.846245	1.828089	-0.911942
C	3.927753	0.425177	-0.360260
C	3.670140	-0.721759	-1.044206
C	3.329139	-0.793383	-2.514569
C	1.811015	-0.829802	-2.767016
C	0.995765	0.085629	-1.880677
Cl	2.503492	-1.343702	2.064440
H	0.294982	4.103324	1.336918
H	0.054935	2.824570	2.554099
H	1.014399	2.489728	1.087496
H	-4.184284	4.355075	-0.694028
H	-4.241785	2.985294	-1.836968
H	-5.066045	2.865599	-0.262582
H	-4.415936	-3.944506	-1.554917
H	-5.216339	-2.549973	-0.784358
H	-4.433652	-2.360610	-2.373588
H	0.152465	-2.941092	1.793518
H	-0.108570	-4.394917	0.782374
H	0.885494	-3.029613	0.187017
H	0.191070	-0.623265	4.325646
H	0.984889	0.523069	3.242279
H	-0.598772	0.943337	4.002520
H	-1.976329	4.507909	0.451183
H	-2.223596	-4.446974	-0.483948
H	2.434398	3.161075	-1.832523
H	2.879934	1.839796	-2.868873
H	3.795445	2.509924	-0.059722
H	4.776425	2.072666	-1.438115
H	3.792779	0.039863	-3.042042
H	3.771444	-1.700479	-2.930817
H	1.598248	-0.602367	-3.818948
H	1.451534	-1.849914	-2.598928

H	-0.070893	-0.134878	-1.895192
H	0.544315	1.998502	-1.130731
H	4.333933	0.322707	0.642217
H	3.866579	-1.658494	-0.529353

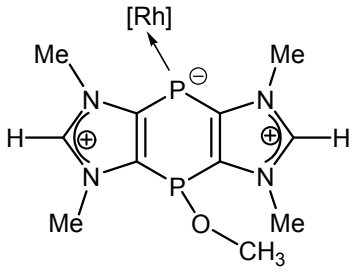

isomer trans: E(M06-2X/6-311+G**) =-2287.665023

C	-1.303325	1.580046	-0.638719
C	-2.483164	1.320652	0.040138
N	-2.982354	2.548931	0.469428
C	-2.153274	3.502632	0.076218
N	-1.140637	2.958894	-0.594913
P	-3.278273	-0.224891	0.520821
O	-2.468462	-0.380594	1.973415
C	-2.652546	-1.580911	2.715478
C	-4.193764	2.748628	1.262899
C	-0.020063	3.700530	-1.182251
P	-0.158788	0.535972	-1.572988
Rh	1.879865	0.224243	-0.156703
C	3.912524	-0.416950	0.402696
C	3.897621	-1.922393	0.527621
C	2.598303	-2.480339	1.136651
C	1.368789	-1.668418	0.751829
C	0.850190	-0.617269	1.509079
C	1.451224	-0.072164	2.786221
C	2.983323	0.074687	2.738804
C	3.478070	0.473300	1.362681
C	-2.306510	-1.234081	-0.632879
C	-1.147888	-0.947117	-1.333916
N	-0.809816	-2.116376	-2.005854
C	-1.719018	-3.055934	-1.745325
N	-2.637422	-2.560319	-0.931739
C	-3.817102	-3.282699	-0.456634

C	0.373559	-2.268456	-2.852372
Cl	2.854490	1.956382	-1.553869
H	0.408645	-3.287444	-3.231982
H	0.313964	-1.559541	-3.678745
H	1.263928	-2.052320	-2.256591
H	-3.820185	-4.275882	-0.901118
H	-3.783539	-3.370627	0.628850
H	-4.715012	-2.743777	-0.755529
H	-4.315902	3.813198	1.451248
H	-5.055473	2.373808	0.712058
H	-4.094448	2.217273	2.209478
H	0.128729	3.361068	-2.207640
H	-0.261660	4.761517	-1.166631
H	0.891720	3.494478	-0.622954
H	-1.708411	-4.060377	-2.138675
H	-2.277268	4.556808	0.268046
H	2.465937	-3.509606	0.795762
H	2.669528	-2.536507	2.224344
H	4.024482	-2.333314	-0.477046
H	4.766768	-2.257210	1.106847
H	3.475008	-0.846729	3.053051
H	3.287969	0.838844	3.456128
H	1.153798	-0.695434	3.639416
H	1.007701	0.912786	2.956137
H	-0.203752	-0.382371	1.383348
H	0.673377	-2.179515	0.090696
H	4.499686	-0.012433	-0.416429
H	3.737875	1.517278	1.214271
H	-2.242505	-1.410841	3.708915
H	-3.714080	-1.838708	2.803267
H	-2.103620	-2.405707	2.246298

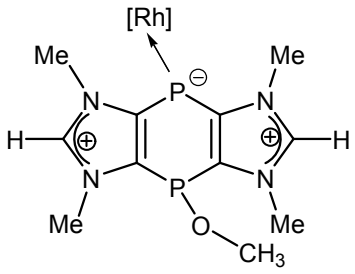

isomer cis: E(M06-2X/6-311+G**) = -2287.664106

C	1.115431	1.281363	-0.800908
N	0.702048	2.577458	-1.087157
C	1.489871	3.444431	-0.450659
N	2.400145	2.777828	0.240653
C	2.198566	1.411813	0.047591
C	-0.456371	2.913353	-1.915470
C	3.481412	3.373446	1.023893
P	3.351373	0.181168	0.684747
O	4.421448	0.279104	-0.585910
C	5.648481	-0.439568	-0.490808
P	0.230617	-0.117484	-1.512672
Rh	-1.968866	-0.106373	-0.298774
C	-1.100256	0.014816	1.643621
C	-1.841175	-0.928695	2.567536
C	-3.363700	-0.955876	2.337005
C	-3.726032	-0.794462	0.873991
C	-4.041912	0.406930	0.276293
C	-4.007038	1.758908	0.948311
C	-2.765050	1.978125	1.830931
C	-1.519584	1.295949	1.281747
C	1.181795	-1.330441	-0.574690
N	0.828901	-2.673621	-0.570851
C	1.652030	-3.342866	0.234009
N	2.534869	-2.506247	0.755786
C	2.281441	-1.222104	0.263554
C	3.581833	-2.875623	1.707350
C	-0.310516	-3.253704	-1.289455
Cl	-2.821129	-1.152468	-2.310750
H	-0.037901	-0.199214	1.540684
H	-0.518967	3.995361	-2.012113
H	-0.336038	2.456670	-2.898320
H	-1.358231	2.515525	-1.442564
H	3.378063	4.456158	0.998296
H	3.416941	3.022641	2.052942
H	4.437937	3.083118	0.588986
H	3.491169	-3.937079	1.929109
H	4.562863	-2.679327	1.275359
H	3.459975	-2.298151	2.622657
H	-0.325542	-2.867813	-2.308827

H	-0.200424	-4.336378	-1.297897
H	-1.240008	-2.955620	-0.803295
H	1.399603	4.518508	-0.494170
H	1.603175	-4.402584	0.429865
H	-2.575903	3.050776	1.911077
H	-2.945170	1.633735	2.850491
H	-4.024279	2.516277	0.160443
H	-4.922983	1.908491	1.532749
H	-3.861529	-0.185633	2.927020
H	-3.757726	-1.909135	2.694120
H	-1.617230	-0.688907	3.614679
H	-1.444312	-1.933457	2.390424
H	-0.748251	1.971585	0.921939
H	-4.550066	0.362684	-0.682485
H	-3.996115	-1.694616	0.329425
H	6.330604	-0.007659	-1.219962
H	6.085490	-0.353701	0.510002
H	5.494468	-1.494283	-0.738987

5. Cyclic voltammetric studies

The electrochemical behaviour in solution of the dicarbenes **4** and **6**$^{cis/trans}$ was investigated by cyclic voltammetry (CV) in THF (0.2 M [$^{n}Bu_4N$][PF_6]) at gold ceramic screen printed electrodes (Au CSPE) [Pine Instruments Company, www.pineinstruments.com]. Voltammetric data was measured in an Ar-filled glove box using the Pine WaveNow potentiostat. The voltammetry results are described first for **6**$^{cis/trans}$ and thereafter for **4** since the former are closely related to previous results on neutral Janus dicarbenes **III** ($R_n = P^{III}NEt_2$) which are expected to behave similarly.[3] Two cyclic voltammetric (CV) experiments on **6**$^{cis/trans}$ mixture have been undertaken in THF with $^{n}Bu_4PF_6$ supporting electrolyte; these compounds are most stable in this solvent and specifically are not stable in CH_2Cl_2, unlike **III**($R_n = P^{III}NEt_2$). Fortunately, CV studies were undertaken on the latter in both CH_2Cl_2 and THF solutions, thus allowing for direct comparisons. In the first set of experiments, a reference compound was not added because of concerns about interference with observed processes and an attempt was made to reference to an immediately proceeding external ferrocene (Fc) experiment for referencing to the $Fc^{0/+}$ = 0 V scale.[4] This attempt was of questionably precision due to a very large ΔE_p > 300 mV for the Fc signal and the inherent uncertainty of external referencing. In a second, shorter, experiment the major scans were repeated and a cobaltocenium salt, [Cc][PF_6], was added as an internal reference, which indeed was found to induce about a 200 mV shift in the process peaks but otherwise displays Nernstian signals.[5] Peak assignments to the (shifted) signals were easily recognizable and are reliably assigned.

The major features of the voltammograms are a series of closely spaced and (chemically) irreversible oxidation steps at facile potentials. These processes are shown in Figs. S35a,b which show almost identical traces when scanned first in the anodic (to +0.25 V) and cathodic (to -2.0 V) directions.

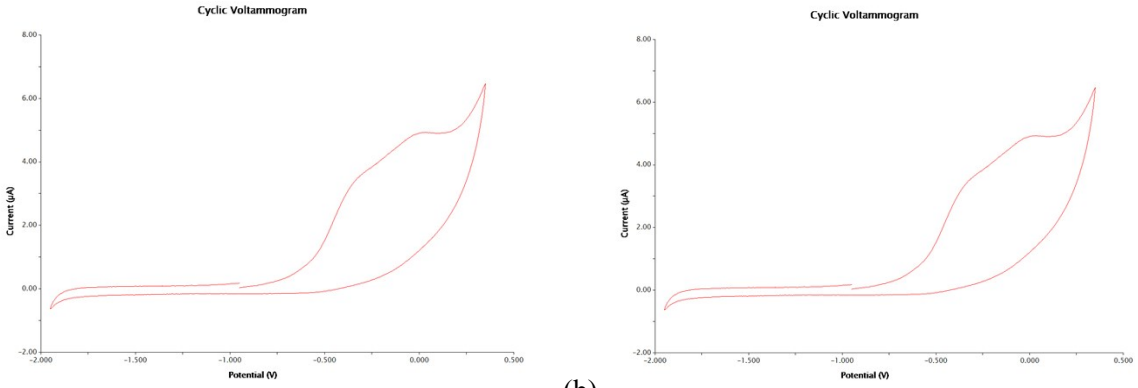

(a) (b)

Figure S35. CVs depicting the primary oxidations of **6**$^{cis/trans}$ in in THF/$^{n}Bu_4PF_6$ medium starting at the OCP scanning (a) first in the anodic and (b) first in the cathodic direction.

Thus, although these are chemically irreversible processes (no return peaks on fast scanning) they appear quite stable within the limited potential range. Moreover, they are facile oxidations commencing at potentials negative of $Fc^{+/0}$ in keeping with previous results from this laboratory and consistent with the electron rich dicarbene nature of **6**$^{cis/trans}$. The multiple oxidations (see below) are attributed to subsequent oxidations of the analyte molecules and not to separate processes for **6**$^{cis/trans}$.

Fig. S36 depicts overlayed CV scans of the full range of accessible processes of **6**$^{cis/trans}$ in this solvent/electrolyte system using ceramic screen-plated Au solid electrodes, along with a background scan showing the experimental solvent window. All potentials are shown on the $Fc^{+/0}$ scale and were referenced with internal [Cc][PF_6] added towards the end of the sequence of experiments. The results with distinct anodic peak potentials E^{a1}_p = -0.29 V and E^{a2}_p = -0.07 V are in broad agreement with those shown for the narrower potential range from the first experiment in Fig. S34. The peak profiles speak to a high likelihood of additional oxidation processes occurring within this potential range. Scans taken more positive than +1.0 V result in major contamination of the working electrode and cannot be analysed, but at least one additional, also irreversible, oxidation could be measured with E^{a3}_p = +0.65.

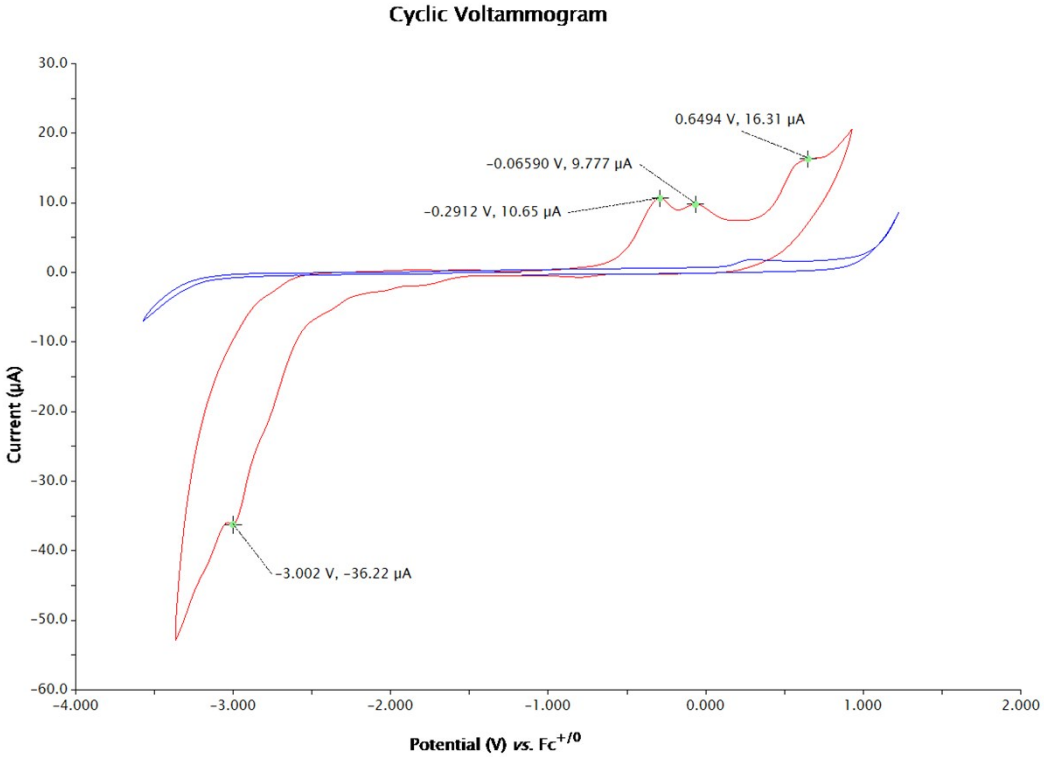

Figure S36. CVs depicting (in blue) the THF/^{n}Bu$_4$PF$_6$ background scan and (in red) the full range of processes for **6**$^{cis/trans}$ accessible in this medium.

Beyond E^{a1}_p and E^{a2}_p, at least one further irreversible oxidation can be measured (E^{a3}_p = +0.65). On scanning in the cathodic direction, the reductive feature E^{c4}_p = -3.00 V is observed which we attribute to some surface-electrode processes, likely from products resulting from the chemically irreversible oxidation processes. The strength of this peak increased strongly with multiple cycles and grows in intensity the longer that experiments are conducted on the sample. Hence, we doubt that under these conditions the true reduction of **6**$^{cis/trans}$ can be measured but it likely exceeds -3.5 V as indicted by the limiting curve visible in Fig. S37 that approaches to the cathodic solvent limit.

These voltammetry results can be interpreted using B3LYP/6-31+G*//M06-2X/6-31+G* computations undertaken with respect to the topologies and energies of the frontier molecular orbitals (FMOs) depicted in Fig. S37. The two highest occupied molecular orbitals (HOMOs) are dominated by carbene σ(p) character, and thus resemble those of **III'** where the substituents at P are Et_2N groups, with either P^{III} or PO^{V} bridging atoms.[3] The P^{III} analogue to **6'**^{cis}

and **6′^{trans}** have HOMO energies, computed at an identical level of theory, of –5.78 and -5.77 eV, so just like **6′$^{cis/trans}$** are virtually identical and likely to be experimentally indistinguishable. (The computed compounds **4′**, **6′^{cis}** and **6′^{trans}** truncate all the linear alkyl substituents to CH_3 to facilitate convergence.) The CV experiments at similar ceramic Au-screen printed electrodes in THF/$^{n}Bu_4PF_6$ for these analogue compounds **III**($R_n = P^{III}NEt_2$) report E^{a1}_p = -0.61 V vs $Fc^{+/0}$; thus the slightly more difficult oxidations E^{a1}_p = -0.29 V for **6′$^{cis/trans}$** are fully consistent with the higher energy HOMOs in the dicarbenes substituted by CH_3O/CH_3 compared to the two Et_2N substituents. The multiple closely spaced oxidation steps fit well with the almost degenerate energies of HOMO and HOMO-1 (i.e. corresponding to the two equivalent C: 'lone pair' electrons). The chemical irreversibility in solution voltammetry is characteristic of such σ-carbene FMOs.[6] In view of (most likely) non-Nernstian character, care must be taken to not over-interpret the significance of the available peak potentials, but experience shows that careful experiments conducted under comparable conditions do give valid results capable of interpretation albeit with lower confidences than Nernstian potentials.

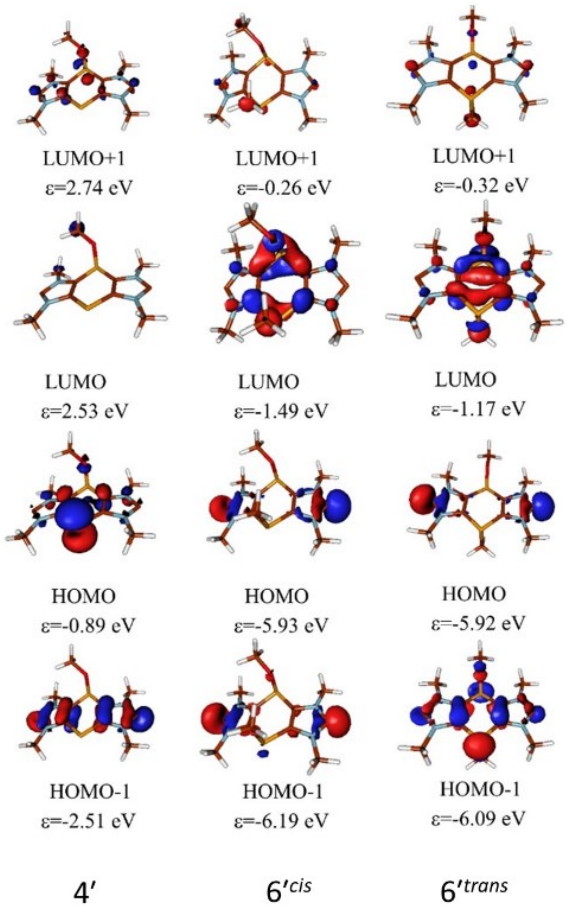

Figure S37. FMO topologies and energies for the model (R = CH_3) calculated structures of **4′**, **6′^{cis}** and **6′^{trans}** at the B3LYP/6-31+G*//M06-2X/6-31+G*level of theory.

The voltammetry of the novel anionic dicarbene **4** was also undertaken twice, first using Fc and later [Cc][PF_6] as reference compounds, although in both cases added *internally*. Whilst in principle, the $Cc^{+/0}$ wave overlaps more of the redox processes of **4** than Fc, it appears that the oxidation of **4** is so facile that by scanning beyond 0 V on the $Fc^{+/0}$ scale as required to actually use Fc as the reference compound, the analyte is destroyed and residues are

deposited on the working electrode that confound further experiments. Hence the analysis here reports the $Cc^{+/0}$-referenced experiments. The key features of the voltammetry of **4** as depicted in Fig. S38 are the very facile first oxidations in a series of small, closely spaced chemically irreversible waves between -1.16 V and -0.74 V, the last of which is the best defined and attributed to E_p^{a5}. The current intensity of these early processes is very small and only the -0.74 V peak approaches the expected peak height for the 1.0 mM analyte. A second set of oxidations can be observed at = -0.36 V and -0.19 V, collectively attributed to E_p^{a6}.

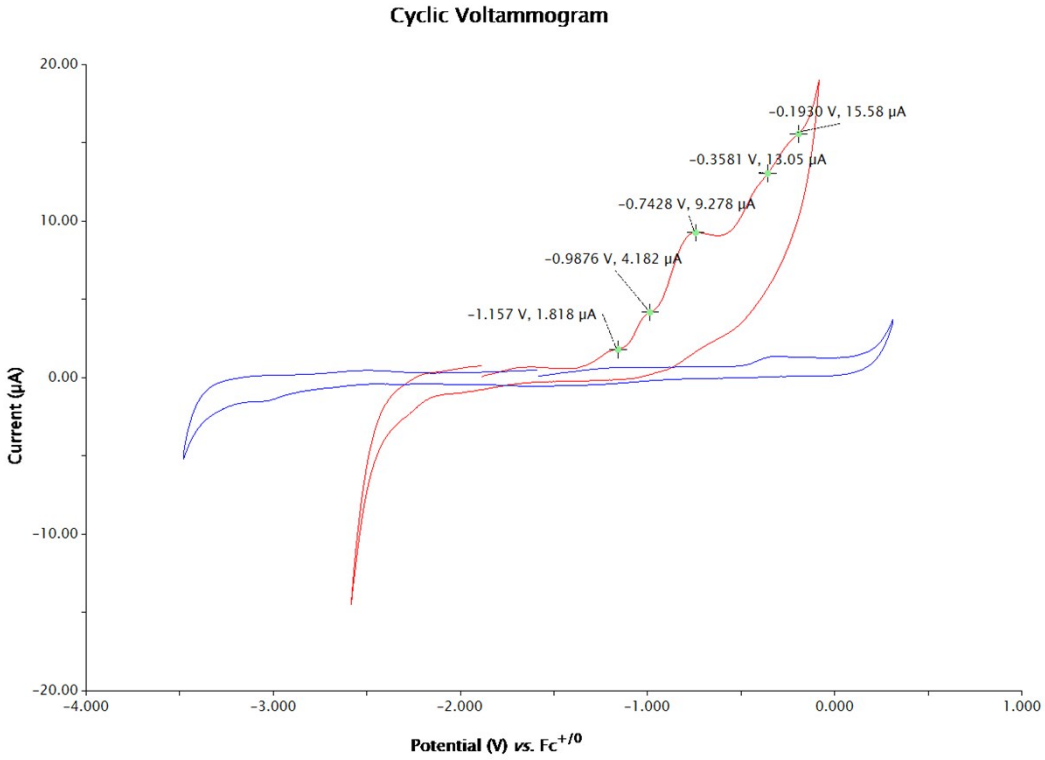

Figure S38. CV (red) of a 1.0 mM solution of **4** (0.2 M) [^{n}Bu$_4$N][PF$_6$] in THF) at 200 mVs^{-1}, and (blue) of the solvent/electrolyte background for the experiment.

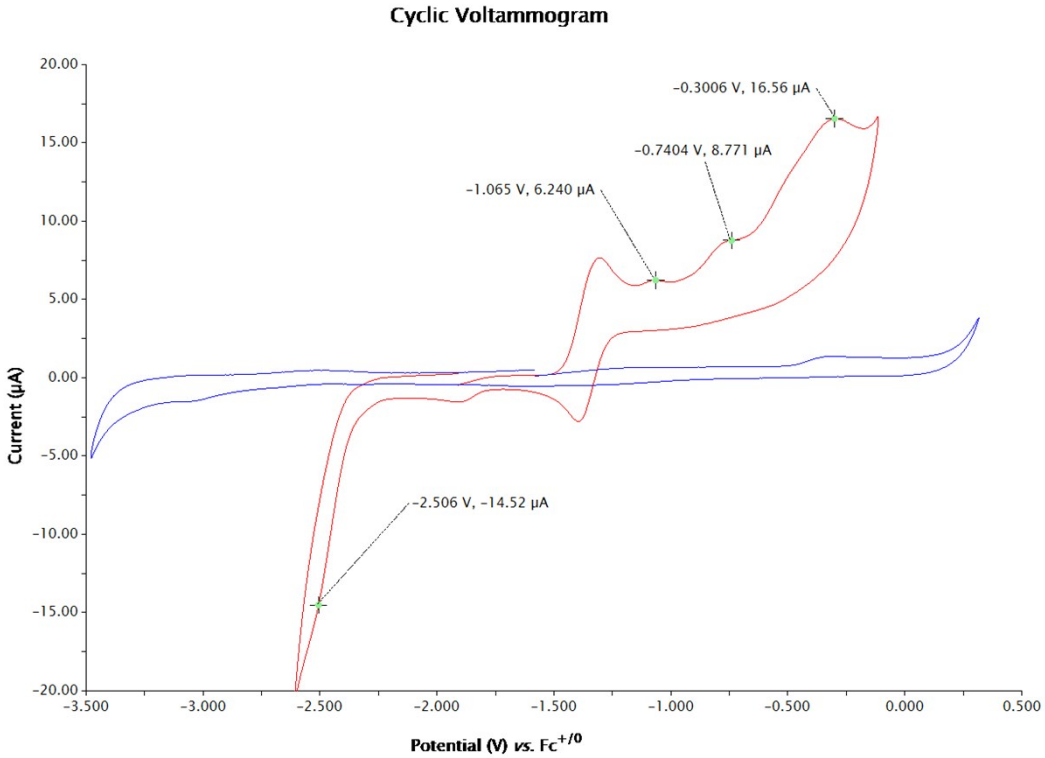

Figure S39. CV (red) of a 1.0 mM solution of **4** (0.2 M [^{n}Bu$_4$N][PF$_6$] in THF) at 100 mVs^{-1} also containing 1.0 mM Cc+/Cc as internal reference, and (blue) background scan for solvent/electrolyte.

In the presence of the added [Cc][PF$_6$] (Fig. S39), which is a well-behaved redox process with ΔE_p ~ 90 mV, the observed oxidation processes are better consolidated. The earliest onset of oxidation appears slightly shifted to -1.07 V. Process E_p^{a5} is easily recognizable at -0.74 V and remains, in our opinion, the dominant first oxidation process. Similarly, E_p^{a6} is better consolidated at -0.30 V. The complex behaviour collectively attributed to E_p^{a5} is much more facile for **4** than is the onset of oxidation in **6**$^{cis/trans}$, whereas E_p^{a6} in the CV of **4** more closely approximates to the first dicarbene oxidation E_p^{a1} in **6**$^{cis/trans}$. As mentioned already, scanning more positive than 0 V vs. Fc$^{+/0}$ leads to sample decomposition with surface contamination. The onset of reduction of **4** labelled as E_p^{c7} around -2.5 V is at least half a volt more facile than E_p^{c4} in **6**$^{cis/trans}$, so that the redox stability window is considerably reduced in the anion.

Naturally, the voltammetry of a P-anionic dicarbene such as **4** should be expected to be complex and sensitive to environmental factors, not the least of which is an interfacial process at a solid gold electrode surface. However, in broad strokes the highly P-centred calculated HOMO of **4′** has a computed energy some 5 eV higher than those of **6'**$^{cis/trans}$ (Fig. S37), whereas the onset of oxidation in solution is only 0.4-1.1 V more facile. Obviously, no direct correlation between the solution voltages and the computed energies is possible when comparing *anionic* **4** with *neutral* **6′**$^{cis/trans}$. This is also obvious from the calculated LUMO energy of **4** which is some 4 eV higher than for the neutral species, whilst the solution reduction appears to have a more facile onset (compare Figs. S38 and S36). Ion pairing of the [Na(cryptand)]$^+$ with P$^-$ in the THF solution is a likely source of energy damping. We also considered alternatives, including fortuitous protonation of reactive **4** under the CV conditions (Fig. S40), which would stabilize

the HOMO in favour of HOMO-1, with standard dicarbene character. This could be disproven by experimental protonation studies which indicate that the sites of protonation are at the carbene (see below).

Nevertheless, if the CVs measured from solutions of **4** truly involved redox processes of this anion, a significantly different response could be expected, with a large separation between the first oxidation to a neutral heterocycle and subsequent oxidation processes. Instead, there is almost no gap between the onset of oxidation and processes that seem to resemble those of dicarbenes, identified here as E_p^{a6}. This is suggestive of an electrochemical step, followed by a fast chemical step (a so-called *EC* process); one-electron oxidation would form a neutral, phosphorus-centred radical **9** (Scheme S1). Such species are known for 1,4-diphosphinines, which rapidly dimerize through a P–P bond resulting in folded structures of very electron rich dimeric heterocycles, i.e. a structure like **10**.[7] It seems reasonable that such a product may undergo multiple low-energy oxidations similar to the carbene oxidations of ***6****cis/trans* consistent with the CVs recorded for **4**, which could be described as an $EC_2(E)^x$ mechanism (where C_2 indicates dimerization).

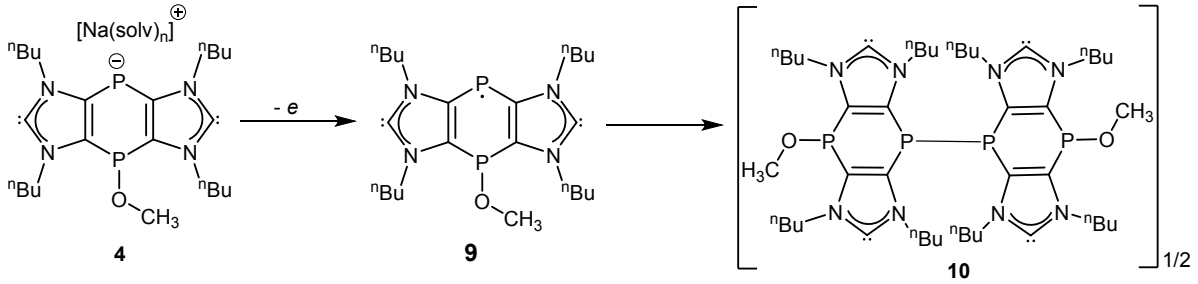

Scheme S1

6. References

[1] M. J. Frisch, G. W. Trucks, H. B. Schlegel, G. E. Scuseria, M. A. Robb, J. R. Cheeseman, G. Scalmani, V. Barone, B. Mennucci, G. A. Petersson, H. Nakatsuji, M. Caricato, X. Li, H. P. Hratchian, A. F. Izmaylov, J. Bloino, G. Zheng, J. L. Sonnenberg, M. Hada, M. Ehara, K. Toyota, R. Fukuda, J. Hasegawa, M. Ishida, T. Nakajima, Y. Honda, O. Kitao, H. Nakai, T. Vreven, J. A. Montgomery Jr., J. E. Peralta, F. Ogliaro, M. Bearpark, J. J. Heyd, E. Brothers, K. N. Kudin, V. N. Staroverov, T. Keith, R. Kobayashi, J. Normand, K. Raghavachari, A. Rendell, J. C. Burant, S. S. Iyengar, J. Tomasi, M. Cossi, N. Rega, J. M. Millam, M. Klene, J. E. Knox, J. B. Cross, V. Bakken, C. Adamo, J. Jaramillo, R. Gomperts, R. E. Stratmann, O. Yazyev, A. J. Austin, R. Cammi, C. Pomelli, J. W. Ochterski, R. L. Martin, K. Morokuma, V. G. Zakrzewski, G. A. Voth, P. Salvador, J. J. Dannenberg, S. Dapprich, A. D. Daniels, O. Farkas, J. B. Foresman, J. V. Ortiz, J. Cioslowski and D. J. Fox, *Gaussian 09, Revision B.01*, Gaussian Inc., Wallingford, CT, 2010, p.

[2] L. Nyulászi, A. Forró and T. Veszprémi, *Phys. Chem. Chem. Phys*., 2000, **2**, 3127 —3129.

[3] N. R. Naz, G. Schnakenburg, A. Mikeházi, Z. Kelemen, L. Nyulászi, R. T. Boeré and R. Streubel; *Chem. Commun*., 2020, **56**, 2646-2649.

[4] G. Gritzner and J. Kuta, *Pure Appl. Chem.* 1984, **56**, 461-466.

[5] The potential for the cobaltocene/cobaltocenium redox couple is known to appear at -1.35 V vs $Fc^{+/0}$ in a wide range of non-aqueous solvents. R. S. Stojanovic and A. M. Bond, *Anal. Chem*. 1993, **65**, 56–64.

[6] (a) M. Feroci, I. Chiarotto, F. D'Anna, F. Gala, R. Noto, L. Ornano, G. Zollo, A. Inesi, *Chem Electro Chem* 2016, **3**, 1133 – 1141. (b) T. Ramnial, I. McKenzie, B. Gorodetsky, E. M. W. Tsang, J. A. C. Clyburne, *Chem. Commun.* 2004, 1054 – 1055.

[7] I. Begum, G. Schnakenburg, Z. Kelemen, L. Nyulázi, R.T. Boeré and R. Streubel, *Chem. Commun.*, 2018, **54**, 13555-13558.